AGU PUBLICATIONS

JGR

Journal of Geophysical Research: Planets

RESEARCH ARTICLE

10.1002/2014JE004622

Special Section:
Results from the first 360 Sols of the Mars Science Laboratory Mission: Bradbury Landing through Yellowknife Bay

Key Points:
- Curiosity has investigated the habitability of Gale Crater, Mars
- Curiosity has explored environments with evidence of ancient fluvial activity
- The unprecedented complexity of the rover challenged science operations

Supporting Information:
- Readme
- Text S1

Correspondence to:
A. R. Vasavada,
ashwin@jpl.nasa.gov

Citation:
Vasavada, A. R., et al. (2014), Overview of the Mars Science Laboratory mission: Bradbury Landing to Yellowknife Bay and beyond, *J. Geophys. Res. Planets*, *119*, 1134–1161, doi:10.1002/2014JE004622.

Received 4 FEB 2014
Accepted 7 MAY 2014
Accepted article online 12 MAY 2014
Published online 5 JUN 2014

Overview of the Mars Science Laboratory mission: Bradbury Landing to Yellowknife Bay and beyond

A. R. Vasavada[1], J. P. Grotzinger[2], R. E. Arvidson[3], F. J. Calef[1], J. A. Crisp[1], S. Gupta[4], J. Hurowitz[5], N. Mangold[6], S. Maurice[7], M. E. Schmidt[8], R. C. Wiens[9], R. M. E. Williams[10], and R. A. Yingst[10]

[1]Jet Propulsion Laboratory, California Institute of Technology, Pasadena, California, USA, [2]Division of Geological and Planetary Sciences, California Institute of Technology, Pasadena, California, USA, [3]Department of Earth and Planetary Sciences, Washington University in St. Louis, St. Louis, Missouri, USA, [4]Department of Earth Science and Engineering, Imperial College London, London, UK, [5]Department of Geosciences, Stony Brook University, Stony Brook, New York, USA, [6]Laboratoire de Planétologie et Géodynamique de Nantes, Nantes, France, [7]Institut de Recherche en Astrophysique et Planétologie, University Paul Sabatier-CNRS-Obs., Toulouse, France, [8]Department of Earth Sciences, Brock University, St. Catharines, Ontario, Canada, [9]Los Alamos National Laboratory, Los Alamos, New Mexico, USA, [10]Planetary Science Institute, Tucson, Arizona, USA

Abstract The Mars Science Laboratory mission reached Bradbury Landing in August 2012. In its first 500 sols, the rover *Curiosity* was commissioned and began its investigation of the habitability of past and present environments within Gale Crater. *Curiosity* traversed eastward toward Glenelg, investigating a boulder with a highly alkaline basaltic composition, encountering numerous exposures of outcropping pebble conglomerate, and sampling aeolian sediment at Rocknest and lacustrine mudstones at Yellowknife Bay. On sol 324, the mission turned its focus southwest, beginning a year-long journey to the lower reaches of Mt. Sharp, with brief stops at the Darwin and Cooperstown waypoints. The unprecedented complexity of the rover and payload systems posed challenges to science operations, as did a number of anomalies. Operational processes were revised to include additional opportunities for advance planning by the science and engineering teams.

1. Introduction

After nearly a decade of design, development, and testing, the Mars Science Laboratory (MSL) mission launched in November 2011 and successfully delivered the rover *Curiosity* to the surface of Mars in August 2012. The mission's scientific focus is the habitability of Mars, primarily as revealed through the geological study of Gale Crater, a site that has retained evidence of aqueous environments in landforms and in the mineralogy of sediments within Aeolis Mons (informally called "Mt. Sharp"), a 5 km high mound at its center [*Grotzinger et al.*, 2012; *Golombek et al.*, 2012]. *Curiosity* addresses habitability also through measurements of the modern atmosphere and environment, by constraining key isotopic ratios that reflect integrated past processes, by revealing how galactic and solar radiation is moderated by the atmosphere, and by advancing the understanding of Mars' meteorology and climatology.

It is precisely the diverse nature of the measurements required to address Mars' habitability that led to the unprecedented scope and complexity of the mission. The mission has 10 scientific payload elements on a roving platform [*Grotzinger et al.*, 2012], together executing the investigations of over 400 international scientists. The payload includes an integrated quadrupole mass spectrometer (QMS), gas chromatograph (GC), tunable laser spectrometer (TLS) that analyzes the atmosphere and evolved gases from samples of rock and soil (SAM) [*Mahaffy et al.*, 2012]; an X-ray diffractometer that determines the mineralogy of those samples (CheMin) [*Blake et al.*, 2012]; focusable medium- and narrow-angle cameras to image the landscape and atmosphere (Mastcam); a laser-induced breakdown spectrometer to remotely sense the chemical composition of rocks and minerals, along with a high-resolution remote micro-imager (ChemCam LIBS and RMI) [*Wiens et al.*, 2012; *Maurice et al.*, 2012]; an arm-mounted camera capable of viewing rock/regolith textures in great detail (MAHLI) [*Edgett et al.*, 2012]; an alpha-particle X-ray spectrometer to determine in situ the chemical composition of rocks and soils (APXS) [*Campbell et al.*, 2012]; an active neutron spectrometer designed to search for water in surface materials (DAN) [*Mitrofanov et al.*, 2012]; a meteorology package to measure modern-day environmental variables (REMS) [*Gómez-Elvira et al.*, 2012]; a sensor designed for

continuous monitoring of background cosmic and solar particle radiation (RAD) [*Hassler et al.*, 2012]; and a descent imager (MARDI).

What most distinguishes this rover mission from those before it is the concept of bringing a laboratory to Mars. A laboratory implies a "bench" in which a diversity of precise experiments can be run under controlled conditions. These controlled conditions extend to the rover's sample acquisition, handling, and processing system [*Anderson et al.*, 2012], where protocols are designed to limit alteration and contamination of samples acquired via scooping or drilling. The laboratory experiments themselves require multiple, iterative runs in order to characterize instrument background and performance, and to optimize the experiments for the questions posed to a particular sample of soil, rock, or atmosphere.

Remote and contact science capabilities are significantly improved over earlier rover missions. ChemCam acquires spectra of rock and soil targets on most sols, resulting in a rich data set of elemental composition and complementing the compositional and mineralogical analyses of the other instruments (which require resource-intensive arm activities to utilize). The third-generation APXS allows a rapid but detailed assessment of elemental composition that also provides key contextual data to studies of acquired samples. The imaging investigations (Mastcam, MAHLI, MARDI, and the remote micro-imager of ChemCam) span scales of microns to kilometers, along with color, stereo, video, and some spectral differentiation. The entire integrated payload has proven to be highly synergistic in accomplishing the mission objectives.

Curiosity's first 500 sols (diurnal cycles) on Mars have met or exceeded established criteria for mission success, in no small part due to the dedication and skill of all those who designed, built, tested, and operate it. The following two sections summarize the milestones and results of the mission from landing through sol 500 (1 January 2014), a significant fraction of the prime mission of one Mars year (669 sols, ending in late June 2014). Following that, mission operations and performance will be discussed, including comparisons with prelanding plans and predictions. While the MSL mission has had its share of challenges, it also has profoundly advanced NASA's scientific approach to Mars exploration, culminating thus far in the first detailed laboratory assessment of a once-habitable environment on Mars.

2. Narrative of the Surface Mission

Curiosity's touchdown was confirmed onboard at 05:17:57.9 Spacecraft Event Time (synced to Coordinated Universal Time) on 6 August 2012, after sensing the touchdown event, firing the cable cutters to release the rover from the descent stage, and waiting 2 s for persistence of contact with the surface. This corresponds to 10:17:57.9 P.M. Pacific Time on 5 August, not accounting for the ~14 min of light time between Mars and Earth, after which the signal was received by the flight team. *Curiosity* touched down at 15:03:09 Local Mean Solar Time on Mars, at 4.5895°S, 137.4417°E, −4501 m elevation, facing an azimuth of 111.5° clockwise from north. The landing location was 2.39 km from the center of the final landing ellipse, located northwest of Mt. Sharp [see *Grotzinger et al.*, 2012, Figure 6]. This landing error is about 0.75σ within the cloud of Monte Carlo landing simulation points (3σ) that spanned 18.6 by 6.4 km (Figure 1). Shortly afterward, the rover acquired images from its front and rear hazard cameras (Hazcams), before deployment of their dust covers. The *2001 Mars Odyssey* (ODY) orbiter remained in communication with *Curiosity* for nearly 6 min after landing, allowing these images to be transmitted to Earth in near real time. After performing critical data management activities, the rover computer transitioned from entry, descent, and landing (EDL) to surface mode, and sol 0 began.

2.1. Commissioning Phase

The Commissioning Phase of the surface mission, spanning the first ~90 sols, was dedicated to a set of activities designed to assess the health and safety of the rover systems and payload elements, and to sequentially bring their full functionality online. Three periods of intensive checkouts and tests, called Characterization Activity Phases (CAPs) 1a, 1b, and 2, were followed by a number of discrete First-Time Activities (FTAs) in which a particular new rover or payload functionality was tested. The CAP activities were rigorously planned, tested, and rehearsed with the operations teams prior to arrival. CAP sequences were uploaded to the spacecraft during cruise, allowing them to be executed with minimal uplink after landing, just a "go" or "no-go" command. Sequences for FTAs were tested and packaged strategically, some before arrival, others as soon as ground testing and approvals were completed. The science team

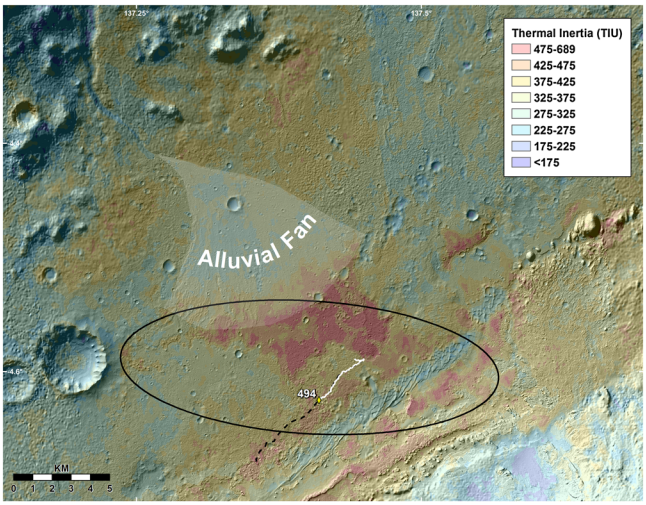

Figure 1. Map of *Curiosity*'s landing site within Gale Crater. A shaded relief map is colorized with thermal inertia derived from the Thermal Emission Imaging System on the ODY orbiter [*Fergason et al.*, 2012]. *Curiosity* touched down at Bradbury Landing (beginning of white line), east-north-east of the center of the landing ellipse. The Peace Vallis alluvial fan spreads across the crater floor north of the landing ellipse. The white line indicates *Curiosity*'s traverse through sol 500, with last motion on sol 494. The dashed line indicates a notional traverse path to the entry point for ascending Mt. Sharp. Image credit: NASA/JPL-Caltech/Arizona State University.

remained engaged during the Commissioning Phase, since it was designed to allow science activities to gradually ramp up over time as various payload elements and rover functions were qualified for nominal use.

2.2. Bradbury Landing

CAP 1a activities began with sol 0 at the landing location, "Bradbury Landing." Along with additional postlanding Hazcam imaging and attitude estimation, the rover fired a number of pyro devices, unlocking the arm, Remote Sensing Mast (RSM), and other hardware from their launch tie-downs in preparation for deployment. On sols 0–3, the team verified the "aliveness" of the payload (i.e., powered on/off), established the high-gain antenna (HGA) link, deployed the RSM, acquired the first Navcam and Mastcam panoramas, characterized the rover's thermal and power systems, and qualified RAD and Mastcam for nominal use. Significant downlink data volume was dedicated to returning EDL data records and the MARDI descent movie (first in thumbnail image format).

Communication with MSL in the first few sols was carried out through the UHF link with ODY and the *Mars Reconnaissance Orbiter* (MRO), with data rates slowly ramped up as they were tested. The HGA used for direct communication to/from Earth was unavailable until the rover's attitude was precisely determined and the steerable antenna deployed and characterized. On sols 4–8, the rover's flight software was upgraded to a new version already on board, optimized for surface operations. CAP 1b followed on sols 9–16, performing health checks of APXS, CheMin, MAHLI, and SAM, and qualifying ChemCam, DAN, and REMS for nominal use. ChemCam obtained its first spectra and image of a Martian rock ("Coronation") on sol 13. CAP 1b ended with a successful unstow of the robotic arm (sol 14) and initial drive (sol 16).

With the capability to drive imminently, the science team spent time during CAP 1 developing a near-term strategy for the surface mission. The slopes of Mt. Sharp beckoned several kilometers to the southwest, but prelanding geologic mapping [*Grotzinger et al.*, 2014] revealed that the rover touched down just west of the intersection of three major terrain types found in the landing area (Figure 2): the hummocky plains (HP) unit upon which the rover landed, a second unit that retains more impact craters than adjacent units, and a bedded, fractured unit characterized by its elevated thermal inertia and its potential relationship to a fluvial system [*Williams et al.*, 2013; *Grotzinger et al.*, 2014]. The fluvial system comprises a channel (Peace Vallis) originating within the northern rim of Gale Crater and terminating in an alluvial fan spreading across the crater floor, including the northern edge of MSL's landing ellipse (Figure 1). While the fan as mapped from orbital images was deemed out of reach given MSL's landing location, its relationship to the light-toned fractured unit made the "triple junction" a compelling destination. The team also considered that the light-toned fractured unit could offer a bedrock target for drilling. The team decided to head east-southeast to the triple-junction site, named "Glenelg," searching along the way for a rock suitable for initial contact science.

With CAP 1 complete and the rover mobile, the Project elected to use a preplanned "intermission" in the Commissioning Phase to drive away from the landing site and to carry out payload activities before starting CAP 2, which was intended to prepare the rover for contact science and sampling. During sols 17–29,

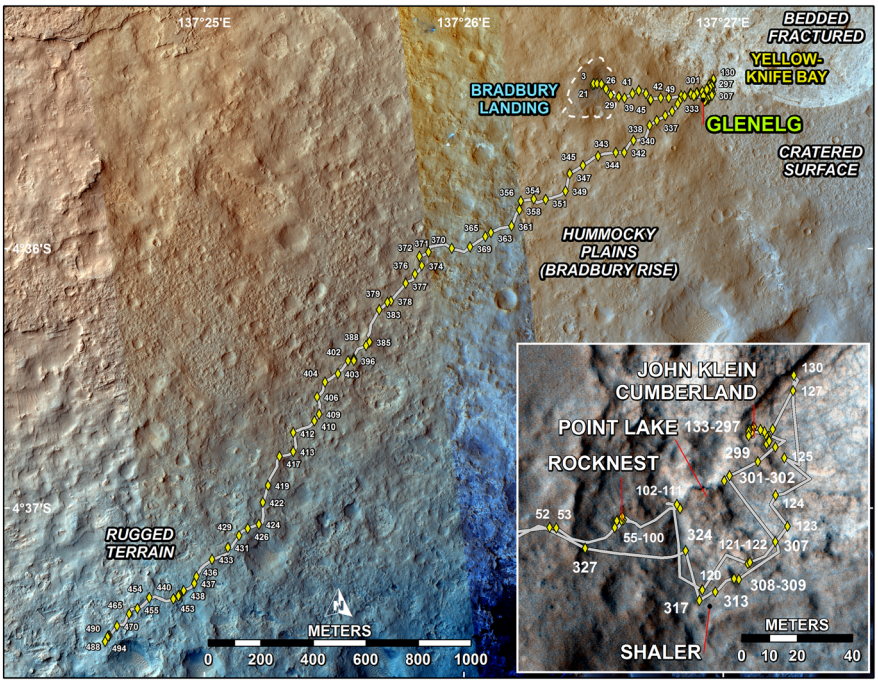

Figure 2. Map of *Curiosity*'s traverses through sol 500. Numbering indicates the sol when each site was reached. Images from the High Resolution Imaging Science Experiment onboard MRO are used for the background. Also marked are the major geologic units (italics) and key locations described in the text. The dashed line around Bradbury Landing indicates the extent of albedo changes associated with landing, presumably caused by removal of dust by landing engine wash. The inset provides a closer look at the Yellowknife Bay region. Image credit: NASA/JPL-Caltech/University of Arizona.

the team completed characterization tests of the MAHLI, Mastcam, ChemCam, and CheMin instruments, while SAM performed its first two analyses of the atmosphere. On sols 20 and 21, the team acquired ChemCam, DAN, and imaging data of "Goulburn," one of the four scours created by the descent engines that revealed underlying bedrock. On sols 26 and 38, the rover came across "Link" and "Hottah," additional bedrock outcrops of conglomerate [*Williams et al.*, 2013].

After *Curiosity* traversed 109 m in six drives (Table 1), CAP 2 executed on sols 30–37. It included checkouts of the robotic arm, sampling tools, and contact science instruments APXS and MAHLI. The MAHLI also was used to acquire a mosaic of the rover's wheels and undercarriage in order to characterize hazards and wear. Some CAP 2 activities required waiting for engineers to assess results before proceeding, leaving time and energy for nominal science activities on most sols (restricted to remote sensing).

2.3. Jake Matijevic and Rocknest Scoop Sample Campaign

Consecutive drives on sols 38–43 brought *Curiosity* to a small, pyramid-shaped rock named "Jake Matijevic" (sometimes shortened to "Jake_M"), chosen for *Curiosity*'s first contact science. Along the way, DAN performed active neutron spectroscopy experiments integrated with the drives. After a short positioning drive on sol 45, Jake Matijevic was analyzed by ChemCam, APXS, and MAHLI on sols 46 and 47, and as the rover departed on sol 48 [*Stolper et al.*, 2013].

As the trek toward Glenelg continued, the team considered how to best accomplish a number of FTAs for the sampling system and analytical laboratories that were required before drilling would be possible. One step was to acquire three samples of particulate material with the scoop. Each scoop would be used to "scrub" the insides of the sample processing chambers and both sides of the 150 μm sieve, reducing contaminants from prelaunch testing or cruise through entrainment and dilution, prior to the first delivery to SAM. Additionally, ChemCam data were acquired routinely along the trek [*Meslin et al.*, 2013].

The science team reasoned that an aeolian bedform would likely contain a well-sorted deposit of loose material, thick enough for scooping, and likely composed of basaltic fines that would not behave or evolve

Table 1. Summary of Rover Traverses and Post-Traverse States

Sol	Drive Number	Distance (m)	Total Odometry (m)	Site Index	Elevation (m)	Azimuth (CW From North)	Comment
0	—	—	—	1	−4501	111.5°	Landing
16	1	7.0	7.0	3	−4501	228.0°	Mobility checkout
21	2	4.9	11.9	3	−4501	195.3°	Drive to Goulburn scour
22	3	15.1	27.0	3	−4502	64.6°	Begin drive to Glenelg
24	4	21.5	48.5	3	−4502	116.5°	
26	5	29.8	78.3	3	−4502	45.2°	
29	6	30.6	108.9	4	−4503	239.8°	Begin break for CAP2
38	7	32.3	141.2	4	−4504	90.6°	Resume drive to Glenelg
39	8	21.7	162.9	4	−4504	85.5°	
40	9	37.2	200.2	4	−4504	89.3°	
41	10	27.0	227.0	4	−4504	89.3°	
42	11	32.0	259.1	4	−4507	109.8°	
43	12	30.0	289.0	4	−4508	82.0°	
45	13	4.5	293.5	4	−4508	124.3°	Approach to Jake Matijevic
48	14	41.7	335.2	4	−4510	171.3°	Resume drive to Glenelg
49	15	30.7	366.0	4	−4511	89.2°	
50	16	48.9	414.9	4	−4515	45.2°	
52	17	36.3	451.2	4	−4517	99.8°	
53	18	2.1	453.3	4	−4517	81.4°	Approach to Bathurst Inlet
55	19	23.5	476.8	4	−4517	0.2°	Arrive at Rocknest
56	20	5.9	482.7	4	−4517	282.5°	
57	21	1.8	484.5	5	−4517	282.8°	Wheel scuff of scoop target
59	22	5.5	490.0	5	−4517	276.7°	Arrive at Rocknest scoop site
100	23	1.9	491.9	5	−4517	272.3°	
102	24	25.3	517.2	5	−4517	87.8°	Drive to Point Lake
111	25	1.9	519.1	5	−4517	56.2°	
120	26	34.6	553.7	5	−4517	45.6°	Drive to Shaler
121	27	24.2	577.9	5	−4518	23.9°	Drive to Yellowknife Bay
122	28	1.0	578.9	5	−4518	65.3°	
123	29	19.4	598.3	5	−4519	36.9°	
124	30	14.0	612.3	5	−4519	32.9°	
125	31	26.1	638.4	5	−4520	269.8°	
127	32	32.8	671.2	5	−4520	45.4°	
130	33	5.6	676.8	5	−4520	324.1°	
133	34	21.7	698.5	5	−4520	214.6°	
147	35	3.0	701.5	5	−4520	202.2°	
151	36	0.7	702.2	5	−4520	204.3°	
152	37	2.4	704.6	5	−4520	200.7°	
159	38	1.4	705.9	5	−4520	223.8°	
162	39	9.0	714.9	5	−4520	220.4°	
163	40	1.9	716.8	5	−4520	221.7°	
164	41	3.2	720.1	5	−4520	200.8°	
166	42	3.3	723.4	5	−4520	165.7°	Arrive at John Klein drill site
272	43	3.1	726.5	6	−4520	200.0°	Drive to Cumberland
274	44	0.7	727.2	6	−4520	200.1°	Arrive at Cumberland drill site
295	45	6.3	733.5	6	−4520	40.9°	
297	46	19.8	753.3	6	−4520	233.6°	DAN traverse
299	47	8.4	761.7	6	−4519	232.4°	DAN traverse
301	48	12.0	773.7	6	−4518	244.4°	DAN traverse, drive to Point Lake
302	49	2.7	776.5	6	−4518	215.1°	
307	50	31.8	808.2	6	−4518	151.1°	Drive to Shaler
308	51	22.0	830.2	6	−4517	234.8°	
309	52	1.8	832.0	6	−4517	270.0°	
313	53	9.3	841.3	6	−4517	104.8°	
317	54	6.8	848.1	6	−4517	160.3°	
324	55	18.0	866.1	6	−4517	166.6°	Begin trek to Mount Sharp
327	56	40.0	906.1	7	−4516	241.0°	
329	57	41.1	947.2	7	−4515	244.3°	
331	58	28.0	975.2	7	−4513	221.1°	
333	59	15.5	990.8	8	−4512	197.7°	

Table 1. (continued)

Sol	Drive Number	Distance (m)	Total Odometry (m)	Site Index	Elevation (m)	Azimuth (CW From North)	Comment
335	60	38.2	1029.0	8	−4510	218.9°	
336	61	32.9	1062.0	8	−4508	239.9°	
337	62	37.7	1099.6	8	−4506	242.1°	
338	63	34.1	1133.7	8	−4504	237.6°	
340	64	100.3	1234.0	8	−4504	242.6°	
342	65	62.4	1296.4	9	−4500	206.7°	
343	66	33.7	1330.1	9	−4500	241.4°	
344	67	70.1	1400.2	9	−4499	240.5°	
345	68	70.2	1470.3	10	−4499	235.2°	
347	69	60.1	1530.5	10	−4499	210.2°	
349	70	70.2	1600.6	10	−4500	209.1°	
351	71	85.1	1685.7	11	−4501	235.0°	
354	72	57.1	1742.8	11	−4500	235.0°	
356	73	50.0	1792.8	11	−4501	205.1°	
358	74	35.0	1827.9	11	−4500	194.1°	
361	75	73.1	1900.9	12	−4501	203.0°	
363	76	84.6	1985.5	12	−4502	215.9°	
365	77	26.5	2012.0	12	−4502	225.1°	
369	78	70.1	2082.1	12	−4503	214.9°	
370	79	81.6	2163.7	13	−4503	209.7°	
371	80	110.2	2273.2	13	−4504	204.1°	
372	81	40.1	2313.9	13	−4503	215.6°	
374	82	42.9	2356.8	14	−4502	207.9°	
376	83	43.0	2399.8	14	−4504	210.8°	
377	84	61.3	2461.1	14	−4503	221.1°	
378	85	90.1	2551.2	14	−4504	222.6°	
379	86	15.1	2566.3	14	−4503	230.1°	
383	87	42.4	2608.8	14	−4504	224.6°	
385	88	141.5	2750.3	15	−4501	186.3°	
388	89	24.3	2774.5	15	−4502	179.4°	
390	90	75.2	2849.7	15	−4507	160.5°	
392	91	2.7	2852.5	16	−4506	141.1°	Arrive at Darwin-1
396	92	9.8	2862.3	16	−4506	173.9°	Arrive at Darwin-2
402	93	22.8	2885.0	16	−4506	260.1°	
403	94	67.9	2953.0	16	−4506	220.7°	
404	95	64.3	3017.2	16	−4504	262.9°	
406	96	72.6	3089.9	16	−4504	210.9°	
409	97	70.6	3160.4	17	−4504	186.1°	
410	98	32.9	3193.4	17	−4503	214.5°	
412	99	97.3	3290.7	17	−4503	217.8°	
413	100	79.8	3370.5	18	−4501	160.2°	
417	101	58.5	3429.0	18	−4499	175.4°	
419	102	125.8	3554.8	18	−4498	179.7°	
422	103	70.0	3624.7	19	−4498	179.3°	
424	104	94.4	3719.2	19	−4498	205.0°	
426	105	47.8	3767.0	19	−4497	205.6°	
429	106	46.4	3813.4	20	−4497	200.7°	
431	107	71.5	3884.9	20	−4496	210.1°	
433	108	93.4	3978.3	20	−4493	221.0°	
436	109	93.5	4071.8	21	−4493	200.2°	
437	110	31.9	4103.7	21	−4492	200.9°	
438	111	48.8	4152.6	21	−4494	211.9°	
439	112	25.5	4178.1	21	−4495	220.1°	
440	113	4.7	4182.8	21	−4495	192.6°	Arrive at Cooperstown
453	114	46.9	4229.7	22	−4493	209.7°	
454	115	103.3	4333.0	22	−4493	211.8°	
455	116	87.2	4420.2	23	−4494	141.3°	
456	117	0.0	4420.2	23	−4494	141.3°	No motion due to fault
465	118	50.3	4470.5	23	−4493	206.4°	
470	119	74.0	4544.5	23	−4492	209.5°	

Table 1. (continued)

Sol	Drive Number	Distance (m)	Total Odometry (m)	Site Index	Elevation (m)	Azimuth (CW From North)	Comment
472	120	50.0	4594.5	24	−4491	215.8°	
474	121	8.7	4603.2	24	−4491	204.7°	
477	122	5.3	4608.4	24	−4491	186.2°	
488	123	0.5	4609.0	24	−4491	186.6°	Wheel imaging campaign
490	124	1.3	4610.2	24	−4491	186.7°	Wheel imaging campaign
494	125	20.2	4630.4	24	−4490	211.6°	

unexpectedly within the sampling system. An aeolian bedform also would likely have a grain size distribution such that a significant fraction would pass through the 150 μm sieve. High-resolution MRO images indicated several aeolian bedforms in the vicinity. On sol 55, the rover arrived at "Rocknest," a site where a group of rocks created a sand shadow displaying a number of bedforms.

Sols 56–101 were spent near the Rocknest site, 400 m (straight-line) and 490 m (odometry) distant from Bradbury Landing (Figure 2). A particular bedform chosen for scooping was scuffed with a wheel to assess its interior. Remote sensing and contact science instruments both studied the deposit from a scientific perspective and confirmed its chemical composition as typical of other Mars soils and therefore safe for sampling [*Blake et al.*, 2013]. The first, third, and fourth scoops were used for decontamination. The second scoop was discarded due to an anomaly unrelated to the sample (section 5). Portions from the third, fourth, and fifth scoops were delivered to CheMin, resulting in the first X-ray diffraction analyses from Mars [*Bish et al.*, 2013]. Four portions from the fifth scoop were delivered to SAM, providing its first evolved gas analyses [*Leshin et al.*, 2013]. Portions from the third and fourth scoops were delivered to the observation tray [*Anderson et al.*, 2012], but imaging revealed that vibration-inducing mechanisms used to promote particulate flow within the sample processing system also were mobilizing material on the tray, causing some of it to migrate off of the tray in the direction of the rover's tilt. Additional investigation of the issue, including a successful APXS analysis of a portion from the fifth scoop on the tray, occurred on sols 95–96. At Rocknest, *Curiosity* acquired its first self-portrait, the product of 55 MAHLI images and a complex series of arm maneuvers, documenting both the rover and the sampling site (product number PIA16239 at NASA's Planetary Photojournal, http://photojournal.jpl.nasa.gov). On sol 102, *Curiosity* executed its first "touch and go," acquiring APXS spectra of a rock target and driving from the Rocknest site. Sols 103–110 consisted primarily of remote sensing in order to simplify planning during the U.S. Thanksgiving holiday, when the science and operations teams took their first days off after landing.

2.4. Yellowknife Bay: John Klein Drill Campaign

As the rover continued toward Glenelg, a number of drill FTAs were interleaved with the drives. The science team worked with the Rover Planners (engineers who operate the rover's mobility and sampling systems) to define a path through the rugged terrain leading down several meters in elevation to the floor of "Yellowknife Bay," a topographic depression with continuous exposures of the light-toned, fractured unit. It became clear that several distinct and laterally extensive bedrock facies cropped out over this relatively short descent. Short detours were made to investigate dark, vuggy rocks at "Point Lake" (sol 102) in addition to well-stratified, cross-bedded sediments at "Shaler" (sol 120).

After this reconnaissance of the local bedrock, the team decided to drive to the floor of Yellowknife Bay, where the facies and stratigraphic relationships between units defining the complete succession (Yellowknife Bay formation [*Grotzinger et al.*, 2014]) would be more apparent. Contact science on key Yellowknife Bay bedrock targets (the "Sheepbed" and "Gillespie Lake" members) was possible on sols 129 and 132. On sol 133, *Curiosity* reached a suitable imaging site and acquired a number of panoramas over the next several sols. On sols 138–139 and 141–146, *Curiosity* ran an onboard "science run-out" sequence consisting of atmospheric imaging and environmental monitoring that freed the planning team for the winter holiday period.

As the team resumed operations in 2013, the priority was to continue investigating the Sheepbed and Gillespie Lake members, with the intent of identifying a target to drill. Sol 147 brought the rover to a thin, linear outcrop for contact science ("Snake River," also called "The Snake"). By sol 157, the team had investigated the Sheepbed and Gillespie Lake contact at a second site.

Having surveyed the geology within Yellowknife Bay, and having discussed how the very fine-grained Sheepbed member may be particularly relevant to a hypothesized, habitable lacustrine setting and would have higher potential for preserving organic materials, the team chose it for *Curiosity*'s first drill-based sample analysis. On sol 162, *Curiosity* drove 8 m toward the team's selected target area. On sols 163–166, the team utilized a wheel to probe one of many ridges observed on some Sheepbed rocks, followed that with contact science on the disrupted area, and completed a short drive to the drill site.

Over sols 166–181, the target "John Klein" (Figure 2) was characterized scientifically and for drill/sampling safety using remote sensing and contact science instruments and by using the drill hardware itself. The sampling system was cleaned (via vibration in various poses), and the analytical laboratories conducted characterization and conditioning activities to prepare for sample analysis. A 20 mm deep test hole was drilled on sol 180. On sol 182, *Curiosity* drilled a 64 mm deep hole, acquiring its first sample of powdered rock. The drill tailings and effect of percussive drilling on the local surface materials were assessed on sols 183 and 184. Remote sensing took place on sols 185–192 while engineers analyzed three unexpected behaviors related to the motor control of the sampling system. Over sols 193–199, the acquired sample was inspected visually using the scoop, sieved, and delivered to CheMin (sol 195) and SAM (sols 195 and 199).

No science operations occurred on sols 201–222 due to a major rover anomaly (section 5). Even after science operations fully resumed on sol 226, rover activities related to the anomaly recovery were given priority. The rapidly approaching solar conjunction period, which would prevent uplink to *Curiosity* for 26 sols, lent a sense of urgency to making sure the rover was in a safe and stable state. In the sols remaining before solar conjunction, additional analyses of John Klein material were performed. The John Klein material remaining in the sample processing system was carefully dumped on the ground so that APXS, MAHLI, and ChemCam could analyze both the sieved and unsieved portions, providing SAM and CheMin with additional information on their delivered samples.

2.5. Yellowknife Bay: Cumberland Drill Campaign

The commanding blackout due to solar conjunction spanned sols 236–261. During this time, *Curiosity* ran an onboard science run-out sequence consisting of environmental monitoring, with two additional sequences on sols 236 and 250 to update the REMS observation schedule table. After planning on sol 262, the science team stood down on sols 263–266 while the rover flight software was upgraded. Over sols 267–273, the team acquired additional observations of the John Klein site and CheMin analyses of the sample material.

The breaks in science planning allowed the team to evaluate the next steps at Yellowknife Bay. Measurements thus far revealed the importance of the Sheepbed mudstone to overall mission objectives (section 3). The team decided to acquire a second sample in order to confirm the results from the first. The "Cumberland" target selected for the follow-on experiment was reached after drives on sols 272 and 274. The Cumberland drill target is 2.75 m from John Klein on similar bedrock but with a higher concentration of nodules [*Vaniman et al.*, 2014], providing the opportunity to measure their composition. A 66 mm drill hole produced a sample of powdered rock on sol 279. Laboratory analyses and additional observations of the Cumberland site occurred on sols 280–294. *Curiosity* left the Cumberland site with sample material cached within the sampling system in order to allow further analyses as initial results were assessed and as ground testing brought new SAM protocols and capabilities online.

2.6. The Traverse to Mt. Sharp

2.6.1. Planning for the Traverse

The framework for the next steps after the initial drilling campaign at Yellowknife Bay was created at an in-person science team meeting in February 2013 (sols 186 and 187, prior to the first drilling results). Three basic options were considered: remain at Yellowknife Bay to investigate the geologic context and stratigraphy in more detail; head toward Mt. Sharp with a series of planned stops at waypoints that might reveal key stratigraphic relationships between units on the crater floor; or head directly to Mt. Sharp. The choice was made difficult by unexpectedly diverse geology around Glenelg, weighed against the long journey (~1 year) to Mt. Sharp. Nevertheless, a consensus plan emerged to acquire a dedicated traverse across the Sheepbed-Gillespie Lake contact with the DAN instrument, to acquire additional remote sensing and contact science observations of two bedrock facies noted on the inbound journey (Point Lake and Shaler), to study the crater-retaining unit from the Shaler location, and then to traverse to Mt. Sharp.

Four potential routes between Yellowknife Bay and the base of Mt. Sharp were developed by a subset of team members and presented for discussion. In preparation for the meeting, the traversability and rate of progress on each was defined using methods similar to those used in assessing candidate landing sites [*Golombek et al.*, 2012; *Arvidson et al.*, 2014]. A "Rapid Transit Route" (RTR) offered the fastest progress (not the shortest distance, since odometry is traded against slower progress on challenging terrain in the analysis). A northern route emphasized the contact between the light-toned fractured unit and the Bradbury Rise region (Figure 2) of the HP unit. A middle route largely followed the RTR but included minor excursions to waypoints representative of the various terrains along the route and showing one or more geologic contacts. A southern route emphasized the dune field, as well as bedrock that might be related to the lower layers of Mt. Sharp. Given that all paths were scientifically interesting, but the middle path was estimated to cost ~20% fewer drive sols, the team chose it.

In subsequent team discussions, four waypoints were chosen that would require only minor deviations from the RTR: "Darwin," a site that offers a window into the stratigraphy within Bradbury Rise; "Cooperstown," with exposures of bedded fractured material similar to that within Yellowknife Bay but distant from it; an unnamed site where the poorly understood striated unit [*Grotzinger et al.*, 2014] is in contact with other plains units; and another unnamed site that allows access to a widespread terrain with "washboard" texture that overlies both plains units and lower Mt. Sharp. A drilling campaign would be considered at one waypoint, while the others would be studied with a few dedicated sols of remote sensing and contact science.

To further expedite the arrival at Mt. Sharp, the team established a goal of commanding a drive on every possible planning cycle, except when at the waypoints. The science team developed a prioritized list of systematic observations that would be slotted in around the drives as possible, mostly focused on documenting the traverse each sol with Navcam, Mastcam, MAHLI (from its stowed position), and MARDI, but also using the ChemCam and DAN instruments to provide constraints on elemental chemistry without having to deploy the arm. These activities typically were possible to accomplish without reducing drive duration on a given sol; when not, they usually were deferred in favor of maximizing the drive. Brief opportunistic science observations including contact science often were possible as well, especially within three-sol weekend plans.

2.6.2. Narrative of the Traverse

Curiosity left Cumberland on sol 295 to accomplish the remaining Glenelg objectives, with the DAN traverse on sols 297–301, Point Lake activities on 303–306, and Shaler activities on sols 313–323. On sol 324, executed 4 July 2013, *Curiosity* began a new phase of the mission, focused on making progress toward Mt. Sharp on the RTR (i.e., the middle route that mostly follows the RTR). In practice, Rover Planners used the latest imaging each sol to fine-tune the path based on local roughness and rock abundance, with the aim of staying within a few tens of meters of the notional RTR. On sols 353, 367, 381, and 415, Cumberland sample material cached within the sampling system was delivered to SAM and analyzed. Analogous experiments run as blanks took place on sols 394, 408, 421, and 428.

ChemCam began a campaign of long-range imaging and reflectance spectra (0.4–0.9 μm) [*Johnson et al.*, 2014], taking advantage of the seasonally clearer atmospheric conditions to view targets up to 10 km away. Features observed with *Curiosity*'s highest-resolution imager (RMI) included light-toned scarps, a putative hematite-bearing ridge [*Fraeman et al.*, 2013], and dune features, allowing comparisons with orbital images of these features but with finer detail.

Curiosity reached the Darwin waypoint on sol 392 (Figure 3), performing remote and contact science on sols 394–395. After a short drive to a second Darwin location on sol 396, additional remote and contact observations were made on sols 398–401. *Curiosity* reached Cooperstown on sol 440 (Figure 3), where remote and contact science measurements were acquired on sols 441–443. Several drives approached or exceeded 100 m along the drive from Shaler to Cooperstown and beyond, as a result of long visibility (for ground-based planning of the bulk of each drive using predrive imagery) and the use of autonavigation in the later portion of each drive (Table 1).

Sols 444–450 were dedicated to upgrading rover's flight software (the third and final upgrade for the prime mission). The transition was unsuccessful, however, and after some additional sols to return to the prior

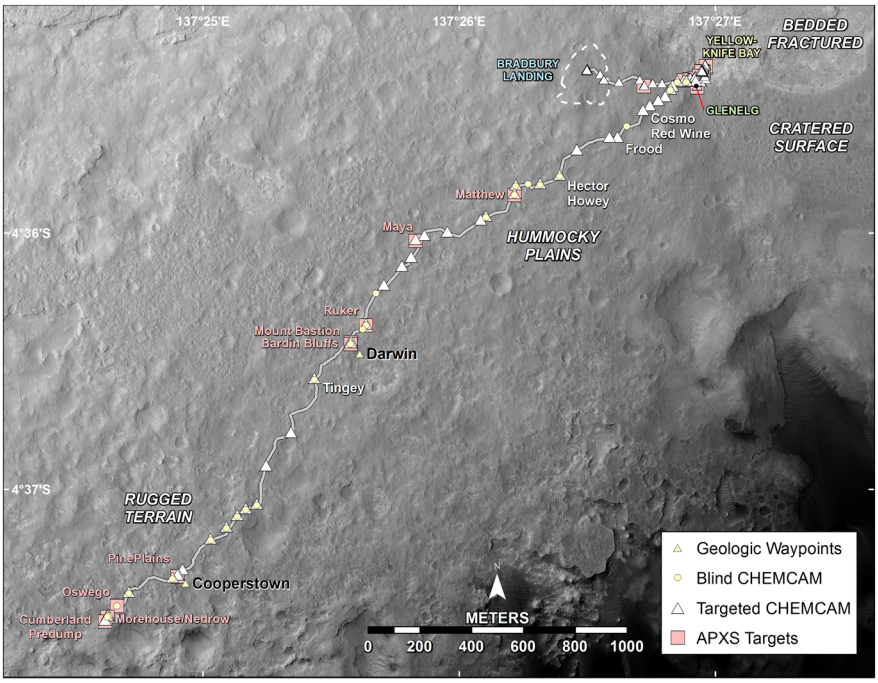

Figure 3. Map of *Curiosity*'s traverses through sol 500 showing the RTR waypoints Darwin and Cooperstown and all ChemCam and APXS targets. Specific targets discussed in this paper are labeled. Blind targeting refers to the use of a fixed geometry when targeting data from the previous sol was not available. Image credit: NASA/JPL-Caltech/University of Arizona.

version, science operations resumed on sol 453. A temporary imbalance in the rover's power bus ceased science operations on sols 458–461. A second and successful attempt to transition the flight software occurred over sols 479–484.

Having completed a number of high-priority SAM experiments on the cached Cumberland material while en route to Mt. Sharp, the team decided to empty the cache in order to simplify arm operations. On sols 463–464, portions of the Cumberland sample were delivered to four SAM sample cups for caching within the instrument. Then the remaining cache of Cumberland sample material was dumped and analyzed with MAHLI and APXS on sols 485–487.

In response to concerns that Curiosity's wheels were being damaged at an unexpectedly high rate (section 5.4), MALHI was used to inventory damage on all wheel surfaces (inside and out) on sols 488 and 490. Sols 495–501 occurred over the winter holidays and included only REMS and RAD monitoring. As of sol 500, *Curiosity* was 3381 m along the RTR from its 4 July position, about 39% of the way to "Murray Buttes," a site marking the entry point to desired traverse routes ascending Mt. Sharp. Total odometry was 4630 m (Table 1).

2.7. Atmospheric Sampling

The SAM QMS and TLS sampled Mars' atmosphere on numerous occasions to assess its chemical and isotopic composition, providing previously unavailable data critical for understanding atmospheric and climate evolution. Air was sampled mostly a few hours after sunset, though some daytime samplings were performed. Early measurements of composition took place on sols 18, 27, 45, and 77 (sometimes executed early on the following sol). Methane was a focus of SAM TLS runs on sols 52, 73, 79, 81, 105, 292, 305, 312, 466, and 474. Other experiments on sols 155, 231, 278, 284, 291, 321, 341, 364, and 434 provided diurnal and seasonal coverage, focused on noble gases, and used additional capabilities within the SAM instrument such as multiple volume expansion (sol 155) and enrichment of lower abundance species using CO_2 and H_2O scrubbers (sols 231, 341, and 364).

2.8. Environmental Monitoring

REMS began operating on sol 1 and initiated its systematic measurements of key meteorological and climatological variables on sol 9. Each sol, a backbone of short hourly sessions (5 min at 1 Hz) is supplemented

by number of full hours (J. Gómez-Elvira et al., Curiosity's Rover Environmental Monitoring Station: the first 100 sols, submitted to *Journal of Geophysical Research*, 2013). The placements of these extended sessions are rotated throughout the sol in order to build up full diurnal coverage every few sols. Occasionally, extended blocks are fixed at specific hours to monitor peak periods of convective vortices or to assess environmental conditions during solid or atmospheric sampling operations. For much of the mission to date, rover energy resources have allowed REMS to acquire six to eight extended sessions each sol, well above the one-session, pre-landing expectation. In response to seasonal changes in energy availability (section 5), after sol 421, the number was reduced to four to five extended sessions.

RAD began operating on sol 1 and has acquired a nearly continuous record of the cosmic ray and energetic particle environment at Mars' surface. Rover energy resources have allowed RAD to run at 100% duty cycle each hour over the full diurnal cycle, relative to a 25% assumption in pre-mission planning. Although RAD and REMS both are designed to operate without the need for the rover CPU (other than for configuration and data transfer), both are required to be powered off for flight software transitions and system-level anomaly recovery. In addition, gaps are present in each data set due to instrument anomalies or instrument-rover communication issues.

The systematic monitoring by RAD and REMS was supplemented by other observations as resources were available. Column dust opacity was measured at roughly weekly intervals through Mastcam imaging of the sun. Opacity measurements and additional REMS extended sessions are aligned with observations of the Gale region by MRO and ODY a few times each week. Other solar and sky imaging characterized dust vertical distribution and optical properties. Navcam was used to acquire short movies every few sols to search for dust devils and orographic clouds, and to measure cloud motions. On many sols, multihour DAN passive measurements were possible, with relevance to both high-energy particle fluxes and surface composition. Finally, ChemCam was used in its passive mode to determine ozone and water vapor column abundances on several sols.

2.9. Astronomical Observations

Curiosity first observed Mars' moons, Phobos and Deimos, in transit across the solar disk on sols 37 and 42, respectively. Other astronomical observations included an occultation of Deimos by Phobos (sol 351), additional Phobos transits (363 and 368), an annular solar eclipse by Phobos (369), an occultation of the star Aldebaran by Phobos (387), and nighttime imaging tests and observations of Phobos, Deimos, stars, and/or Jupiter (378, 385, 393, and 474). Sols 408 and 474 included nighttime opacity measurements (using stars at different airmasses). Over the mission, these observations and others will refine knowledge of the moons' orbits, which in turn will constrain models of Mars' interior. After a test on sol 397, imaging of comet ISON was attempted on sol 408, but the comet was not detected.

3. Science Highlights

Overviews of major findings from Rocknest and Yellowknife Bay have accompanied papers describing those sampling campaigns [*Grotzinger*, 2013, 2014; *Grotzinger et al*., 2014]. A number of other results appear in this issue as companion papers. Below we summarize key findings from *Curiosity*'s operations through Yellowknife Bay and present new results from subsequent exploration along the RTR.

3.1. Highlights from Bradbury Landing Through Yellowknife Bay

The first outcrops encountered by *Curiosity* were sedimentary conglomerates, with sand grains and cemented, rounded pebbles indicating substantial fluvial abrasion [*Williams et al*., 2013]. Regular sampling of rocks and soils by ChemCam has provided information on the variability of surface materials, including a coarse soil fraction whose felsic composition suggests it originated from the breakdown of larger felsic clasts observed along the traverse [*Meslin et al*., 2013; *Ollila et al*., 2014]. The highly alkaline basaltic composition of Jake Matijevic suggests greater fractionation in Mars' upper mantle than previously thought [*Stolper et al*., 2013].

At Rocknest, *Curiosity* analyzed a small deposit of windblown fines [*Blake et al*., 2013; *Minitti et al*., 2013], finding a basaltic composition typical of soils measured at other sites on Mars, though with a significant noncrystalline component that likely is enhanced in volatile species such as H_2O, SO_2, CO_2, and O_2 [*Bish et al*., 2013; *Blake et al*., 2013; *Leshin et al*., 2013; *Archer et al*., 2014; *McAdam et al*., 2014; *Glavin et al*., 2013].

The detection of oxychlorine compounds, such as perchlorates, suggests that their accumulation may be driven by a global process. Considering this global connection, the APXS observation within the wheel scuff ("Portage," sol 89) and Rocknest laboratory analyses are the mission's best references for comparison with soils studied by other landed missions.

The primary science objective of the MSL mission is to quantitatively assess the past and present habitability of environments accessed by the mission. The first in-depth assessment took place at Yellowknife Bay, where fine-grained sedimentary rocks were inferred to be deposited within an ancient lake with associated stream and groundwater systems [*Grotzinger et al.*, 2014]. Analyses of the Sheepbed mudstone [*Grotzinger et al.*, 2014; *McLennan et al.*, 2014; *Ming et al.*, 2014; *Vaniman et al.*, 2014] suggest a sustained (hundreds to tens of thousands of years) aqueous environment characterized by neutral pH, low salinity, variable redox states of both iron and sulfur species, and the presence of key chemical elements such as C, H, O, S, N, and P.

Farley et al. [2014] describe the radiometric and exposure ages determined in situ from radiogenic and cosmogenic noble gases in the Cumberland sample of the Sheepbed mudstone. The geologic context and the exposure age of 78 ± 30 Ma are used to infer a surface erosion rate controlled by wind-driven scarp retreat. Measurements of galactic and solar particle radiation at Mars' surface [*Hassler et al.*, 2014] not only provide key inputs for future human exploration but also underscore the importance of radiation and exposure age in strategies for identifying sites with potential of preserving ancient organic biomarkers.

Measurements of the chemical and isotopic composition of Mars' atmosphere by the SAM instrument have provided an upper limit on the CH_4 abundance (essentially consistent with zero in spring to late summer at Gale Crater) and provided new constraints on early, massive atmospheric loss [*Webster et al.*, 2013a; *Webster et al.*, 2013b; *Mahaffy et al.*, 2013; *Atreya et al.*, 2013; *Wong et al.*, 2013].

Highlights of REMS results include characterization of atmospheric pressure over convective, diurnal, and seasonal time scales, and the first measurements of UV flux and relative humidity from the Martian surface [*Haberle et al.*, 2014; *Harri et al.*, 2014; J. Gómez-Elvira et al., submitted manuscript, 2013]. Ground temperature measurements from REMS vary with the observed geology, such as the higher apparent thermal inertia of the light-toned fractured unit at Yellowknife Bay relative to the plains materials [*Hamilton et al.*, 2014; G. Martinez et al., Surface energy budget and thermal inertia at Gale Crater: Calculations from ground-based measurements, submitted to the *Journal of Geophysical Research*, 2014].

3.2. Initial ChemCam Results Along the RTR

ChemCam was used during the traverse of the HP unit to sample soils, clasts, and bedrock exposures. We focus here on bedrock observations obtained during sols 330–360, leaving subsequent observations at Darwin and Cooperstown to future papers. "Red Wine" (Figure 4a, sol 339) is one of the more definitive bedrock exposures encountered after the rover left Yellowknife Bay. Mastcam imaging shows clasts embedded in a cemented material, similar to the conglomerates observed between Bradbury Landing and Yellowknife Bay [*Williams et al.*, 2013] but with a higher number of dark angular clasts. This target was 6.5 m from ChemCam, near the maximum range of 7 m and not permitting the best quantitative assessment. Nevertheless, several less well exposed pieces of bedrock were present along this section of the traverse and analyzed at "Cosmo" (Figures 4b and 4c, sol 339), "Howey" (Figures 4d and 4e, sol 353), "Hector" (Figures 4f and 4g, sol 353) and "Frood" 1 and 2 (Figures 4h–4j, sol 343). These targets show exposures of conglomerates with various proportions of light-toned and dark-toned material. Local rounded pebbles exist, especially at Frood (Figures 4i and 4j), suggesting the origin of these conglomerates is similar to the fluvial sediments observed at Goulburn, Link, and Hottah [*Williams et al.*, 2013], but the lack of well-exposed sections limits the interpretation.

The compositions extracted from ChemCam partial least squares model [*Wiens et al.*, 2013] show a large variation in chemistry (Figure 5). Compared with Link, which was of intermediate composition including abundant feldspars, several locations in the five targets discussed here display relatively high Al and alkali elements (Na and K), suggesting enrichment in alkali feldspars. For example, the second location of Frood 1 displays light-toned spots in the post-LIBS RMI image (Figure 4j). This location has the highest Al and alkali content, suggesting the laser hit an alkali feldspar gravel (Figures 5a and 5b, point F2). Several other points have much lower proportions of Al-alkalis and relatively more Fe. For example, the third point of the

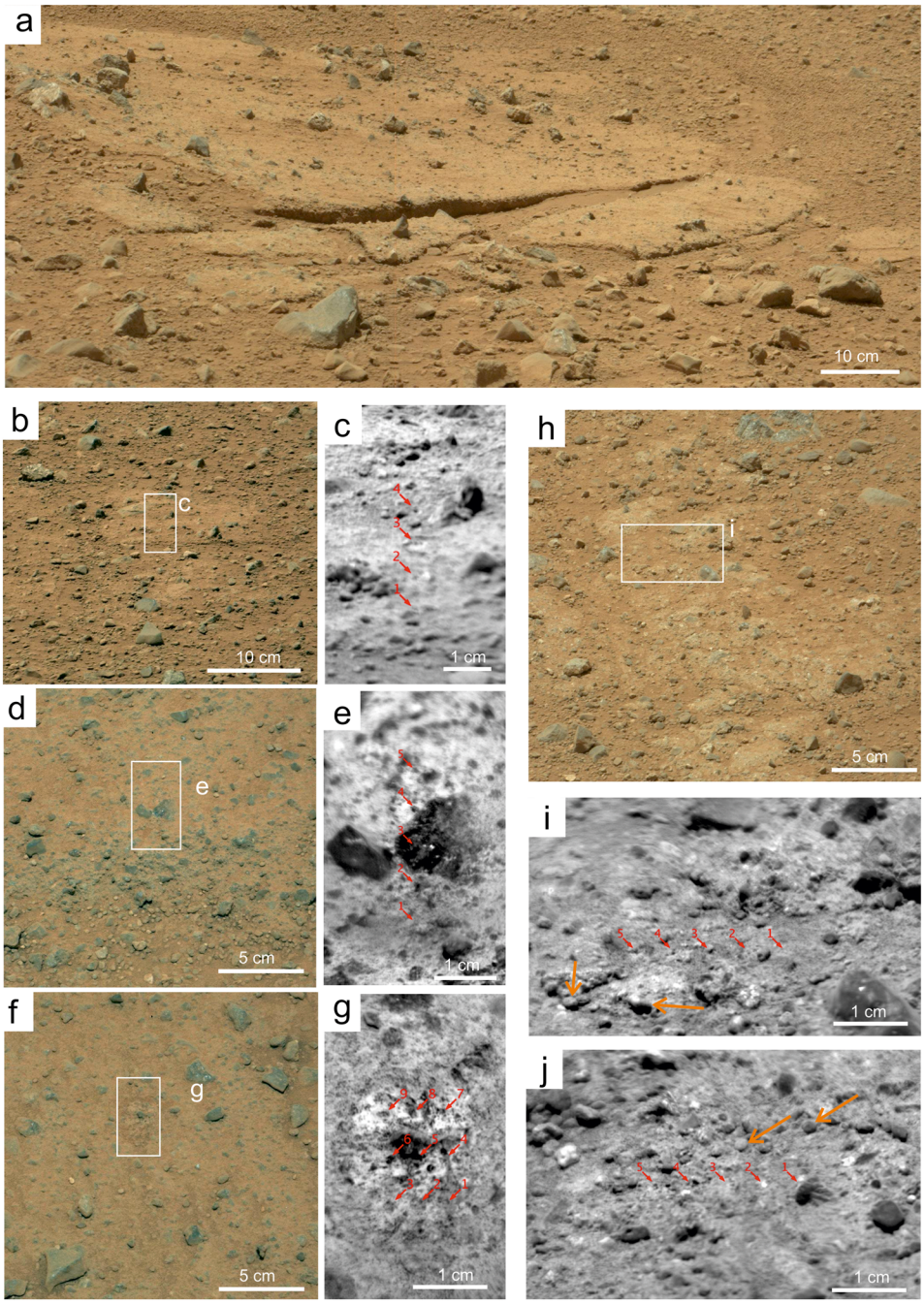

Figure 4. (a) Mastcam image (0339MR1375000000E1_DXXX and 0339MR1375001000E1) of the target Red Wine (sol 339), displaying clasts cemented in an indurated conglomerate. (b) Mastcam image (0339MR1380000000E1_DXXX) of the target Cosmo (sol 339) showing a marginally outcropping bedrock. (c) RMI image (CR0_427590058EDR_F0080610CCAM03339M) of Cosmo. Red arrows indicate individual LIBS shots. (d) Mastcam image (0353MR1445001000E1_DXXX) of the target Howey (sol 353). The 2 cm sized pebbles are dark, and one of them has been analyzed on the third point of the raster, as shown in the RMI image. (e) RMI image (CR0_428826753EDR_F0110302CCAM02353M) of Howey. (f) Mastcam image (0353MR1444001000E1_DXXX) of the target Hector showing similar poorly exposed bedrock. (g) RMI image (CR0_428826049EDR_F0110302CCAM01353M) of Hector. (h) Mastcam image (0343MR1389000000E1_DXXX) of the Frood 2 target showing various clast colors. (i) RMI image (CR0_427940920EDR_F0090236CCAM01343M) of Frood 2, and (j) RMI image CR0_427941742EDR_F0090236CCAM02343M) of Frood 1. The orange arrows show small well-rounded pebbles either cemented in the conglomerate, shown in Figure 4i, or weathered out, shown in Figure 4j. The second point of Frood 1 in Figure 4j displays a light tone.

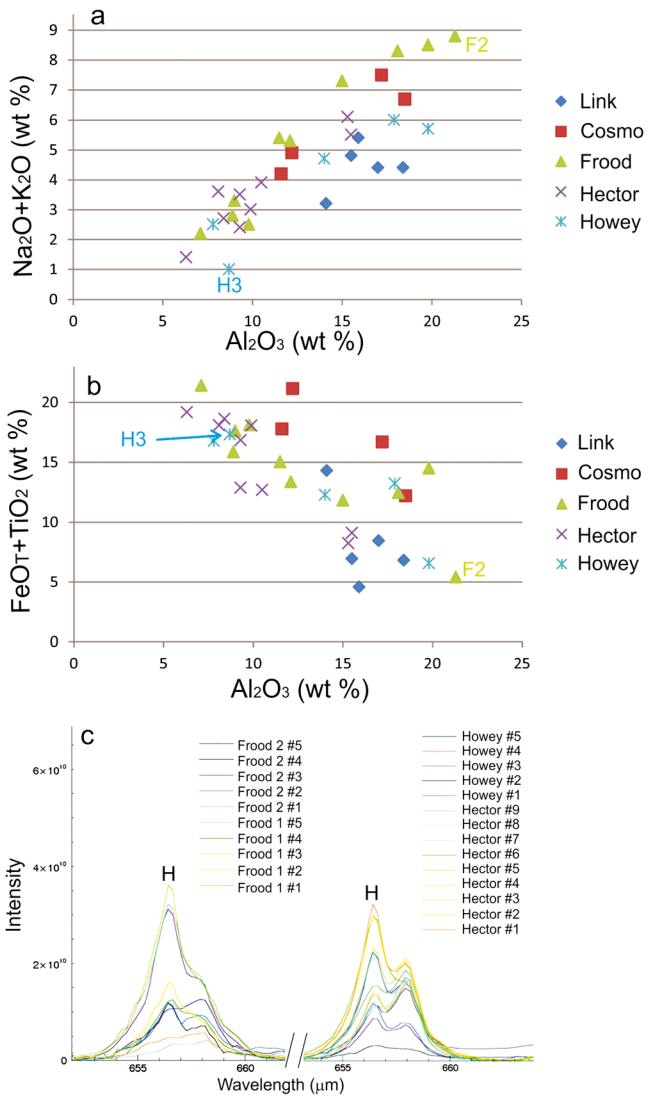

Figure 5. (a) ChemCam compositions showing alkalis versus Al as weight % oxide. (b) Plot of Fe versus Al of the same points. H3 is the third location of target Howey. F2 is the second location of target Frood 1. (c) Emission line of H (656 nm) for the targets Frood, Hector, and Howey. The variable intensity of the H line among locations and targets of conglomerate suggests various levels of hydration within undetermined mineral phases.

target Howey is located on a dark clast (Figure 4e, location 3), which has a predominant mafic composition (Figures 5a and 5b, point H3). The presence of both end-members in these data show that the conglomerates are composed of gravels of coarse texture and various compositions, consistent with igneous rocks from the crater rim transported downslope. They contain feldspar-rich pebbles and are thus more differentiated than usually found on Mars [*Sautter et al.*, 2014]. This is exemplified by the targets Frood 1 and 2; the 10 locations are spread across the whole compositional map (Figure 5). The images display a large diversity in tone, consistent with this compositional variability.

Another notable observation is the presence of hydrogen in many outcrops (Figure 5c), where it may indicate the occurrence of hydrous minerals such as those found in the conglomerate Link and interpreted to be preferentially Fe-rich cements [*Williams et al.*, 2013]. The variable intensity of the H line among the measurements on the conglomerates suggests various levels of hydration. Quantification of H in LIBS analyses is challenging due to "matrix effects" (i.e., effects that depend on the targets' optical and mechanical properties). ChemCam data throughout the traverse indicate that H is relatively high for soils and dust [*Meslin et al.*, 2013], but images of the targets here clearly show the material to be cemented. Spectra from these conglomerates display the most obvious H lines of any rocks analyzed so far at Gale Crater. It is not possible to determine the nature of the hydrous phase(s) present, and if they are present as cements or as previously formed fine-grained material transported by fluvial flows. Future work will further detail the identification of hydrogen in sediments and sort out its origin.

The target "Tingey" (Figure 3, sol 409) is a raster of five points on the surface of an outcrop crossed by a light-toned vein (Figure 6). The rock is likely sedimentary, but a thin cover of soil and pebbles limits our ability to assess whether it is a conglomerate or sandstone, for example. Pebbles on the surface were hit on four of five locations. The third location sampled light-toned material (Figure 6b). The spectra of the third point show strong calcium emission lines, whereas other major elements are strongly depleted or totally absent (as shown for Si, Mg, and Al in Figure 6a). Only sulfur lines are correlated with these calcium lines while oxygen lines are present too (not represented in Figure 6). These observations point toward the presence of calcium sulfates, likely anhydrite, as hydrogen is very low.

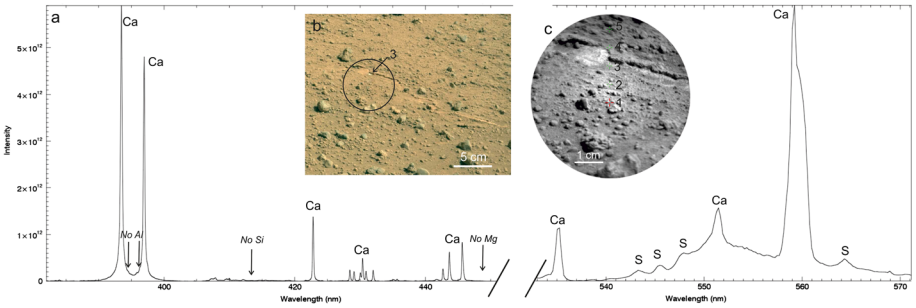

Figure 6. (a) ChemCam spectrum of the third point on target Tingey. (b) Mastcam image (0407MR1685000000E_DXXX) with arrow indicating the point shown in the spectra. The image was taken after the ChemCam shots, showing lighter-toned material after dust was blown away. (c) RMI image of Tingey (CR0_433631492EDR_F0170000CCAM01407M1) showing the location of the five points, with the third one on the light-toned material. This image was taken before the laser shots.

3.3. Outcrop Studies at Shaler, Darwin, and Cooperstown

Characterization of rock outcrops along the RTR reveals the variability of lithologies and sedimentary facies, establishes stratigraphic relationships, and helps reconstruct depositional processes and paleoenvironments. Imaging suggests that similar sedimentary facies are present in rock outcrops across the Bradbury Rise region. Patchy outcrops of varying conglomerate and pebbly sandstone facies are observed extensively on the HP unit. Data presented here indicate that these facies also are abundant in the Rugged Terrain (RT) geomorphic unit, located west of Bradbury Rise and HP (Figure 3). *Curiosity* conducted detailed observations, including contact science, at three significant outcrops: Shaler (Figure 2), Darwin, and Cooperstown (Figure 3).

The ~0.7 m thick, ~20 m wide Shaler outcrop is within the upper Glenelg member of the Yellowknife Bay formation [*Grotzinger et al.*, 2014]. Shaler is characterized by cross-stratified, pebbly sandstones with interbedded, recessive, likely finer-grained intervals (Figure 7) [*Edgar et al.*, 2014]. Shaler strata infill three small (5–10 m wide), shallow paleotopographic depressions. Distinct sediment packages have been identified, typically with upward fining sequences, with some beds that can be traced continuously for more than 20 m. Coarser-grained beds define the base of multiple fining-up sequences. The pebbly sandstone facies exhibits well-developed decimeter-scale trough cross-stratification. Toward the top of the outcrop, a resistant cross-stratified unit is present with a distinct geochemical signature. ChemCam analyses of the Shaler target are consistent with a basaltic composition, with the upper resistant facies displaying high K_2O and elevated Na_2O, Al_2O_3, and SiO_2 [*Anderson et al.*, 2014].

On sol 394, *Curiosity* arrived at Darwin, a stratified sedimentary rock outcrop (Figures 3 and 8). The outcrop was imaged in detail by Mastcam to provide stratigraphic context. APXS and MAHLI observations were made at two locations: first at a ~20 cm thick scarp (Figure 8, parking spot #1), and later at a vein-rich, low-relief outcrop located 4.6 m from the initial location (parking spot #2). The Darwin outcrop is characterized by interbedded packages of light-toned, fine-grained sandstone and darker pebbly sandstones [*Williams et al.*, 2014; *Yingst et al.*, 2014]. At the first location, a basal unit targeted as "Altar Mountain" is a poorly sorted, pebble-rich sandstone facies, comprising sand and pebble clasts ranging from <1 mm to 22.4 mm in diameter. Clasts are subangular to subrounded in shape. The facies is grain supported, poorly

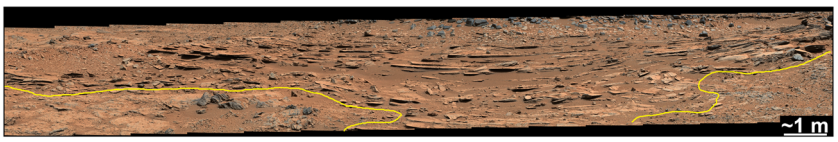

Figure 7. Mastcam mosaic of the Shaler outcrop acquired on sol 120, during *Curiosity*'s first visit to Shaler on approach to Yellowknife Bay. Yellow lines mark the contact between Shaler and the underlying Gillespie sandstone. There are several outcrop-length surfaces that represent gravel-rich deposits that fine upward. These surfaces enable correlation of distinct sediment packages across the outcrop. Image credit: NASA/JPL-Caltech/MSSS.

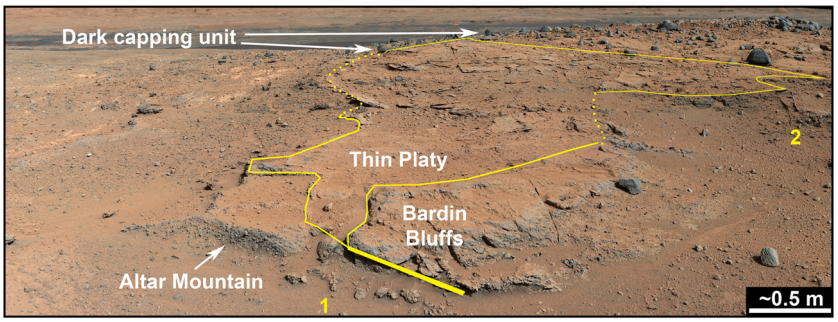

Figure 8. Sketch map of facies contacts in the Darwin outcrop, with the approximate locations of the two parking sites marked by numbers, on this Mastcam mosaic acquired on sol 390. Four distinct facies are noted. Image credit: NASA/JPL-Caltech /MSSS.

sorted, and shows no preferred grain orientation. No clear grain imbrication is apparent. Pebbles are observed to be floating in a sandstone matrix. Clasts commonly show evidence for surface pitting.

Overlying the Altar Mountain bed is the "Bardin Bluffs" target, which also comprises a pebbly sandstone bed, though with an apparently greater proportion of larger clasts. It forms a generally structureless bed, though it appears to show some fining upward. Some fine pebbles (<1 cm in diameter) in Bardin Bluffs are rounded; others exhibit pockmarks and hairline fractures (Figure 9). Highest-available resolution images show angular fragments embedded in rounded pebbles, surrounded by a matrix component that displays flow banding (Figure 9b). Thin sandstone plates are interbedded with the other facies. Dark blue-gray, resistant-pitted rocks cap the outcrop and may be similar to the dark resistant facies at Shaler, though were not investigated in detail here.

The Darwin outcrop is well lithified and heavily fractured. There is a prominent, localized fracture set (Figure 10) that was the target of investigation at the second contact science site. The filled fractures, interpreted as veins, are defined by closely spaced, approximately parallel ridges that cross-cut the lower facies and thin, platy strata. Individual ridges extend ~2 m long, and the assemblage spans ~ 0.5 m. Discrete fine pebbles are bound within the vein-filling material and are especially prominent on the surface of the vein ridge top, where they are more resistant to weathering. ChemCam analyses of targets on the veins detected enrichment of Si and Al, consistent with a feldspathic composition. The ChemCam data are suggestive of a silica cement in the Darwin veins.

APXS spectra from cobble and matrix targets examined at Bardin Bluffs have lower MgO, K_2O, P_2O_5, TiO_2, and Ni than those examined at the second stop (eight targets, including an analysis called "Mount Bastion").

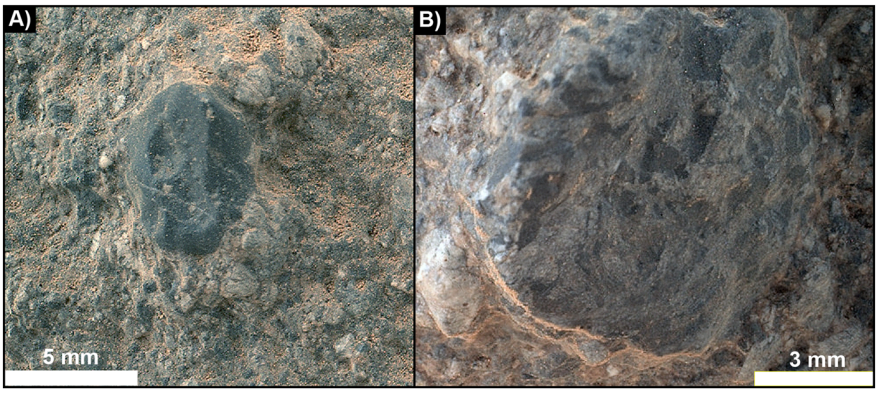

Figure 9. MAHLI images of the Darwin outcrop acquired on sol 394. (a) Pock-marked clast in Bardin Bluffs facies. (b) MAHLI image of a clast embedded in the pebbly sandstone target Bardin Bluffs. Note the variation in angularity among the fragments within the clast surrounded by a matrix component with apparent flow banding. Image credit: NASA/JPL-Caltech /MSSS.

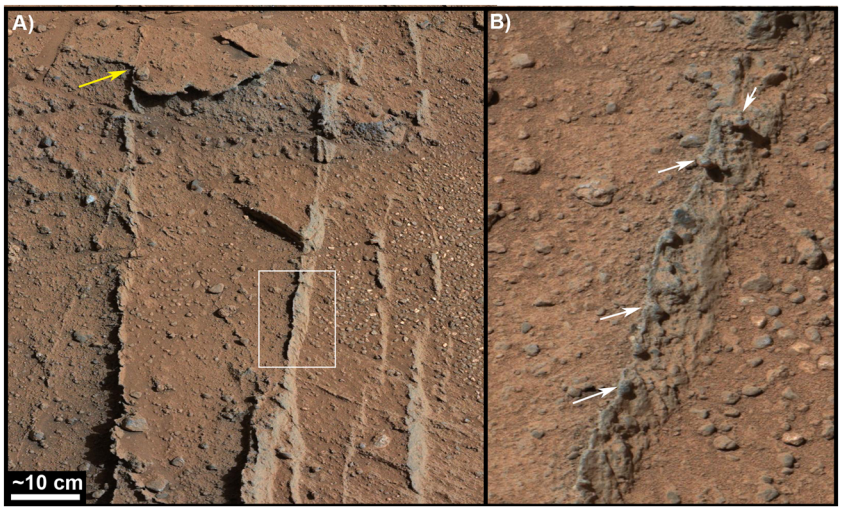

Figure 10. (a) The veins at Darwin site 2 (see Figure 8 for location) are closely spaced and nearly parallel. Veins cross-cut several facies, including the thin, platy facies at the yellow arrow that hosts the Mt. Bastion target. Mastcam image acquired on the afternoon sol 396. (b) Pebbles along the ridge crest are marked by white arrows. Mastcam image acquired on the morning of sol 401. The different illumination conditions cause the vein to appear lighter or darker than the surrounding surface.

Outcrop at the second Darwin stop was much dustier than the first stop, with SO_3 ranging to 7.8 wt%, greater than the SO_3 of the dusty soil Portage from sol 89 [*Schmidt et al.*, 2014a]. No discernable difference in APXS composition was detected between cobbles, matrix, and through-going vein material.

Cooperstown is a well-exposed sedimentary rock outcrop that is capped by a ~50 m long, 0.2 m high escarpment formed by a more-resistant, well-cemented bed (Figure 11). The outcrop is characterized by sandstone and pebbly sandstones. The strata are approximately subhorizontal and can be traced laterally across the outcrop. Individual beds define a general coarsening upward succession. The basal facies comprise thin-bedded cross-stratified sandstones. These are overlain by a distinct, structureless sandstone, studied at "Rensselaer." This sandstone is fairly well sorted, comprising subrounded, medium to coarse sand grains, though the well-developed cementation makes it difficult to identify individual grains. The sandstone is characterized by isolated floating pebbles in the sandstone matrix, in particular very distinct elongate, platy clasts and hollows (where clasts have eroded out) that resemble mudstone intraclast conglomerates commonly observed in fluvial deposits on Earth.

APXS spectra from Rensselaer and "Pine Plains" (sols 441 and 442) show high K_2O (up to 2.5 wt%) and MgO (up to 8.7 wt%), and low SiO_2 (down to 41.7 wt%). Similarity in APXS compositions (Figure 12) link Cooperstown targets to Bathurst Inlet (sol 54). In addition, two targets of opportunity along the rover's traverse, including "Oswego" (sol 472) and the substrate rock onto which the cached Cumberland sample was dumped (sol 485), also share compositional characteristics with Bathurst Inlet, indicating that the Bathurst Inlet class rocks are relatively widespread in the RT unit first encountered around sol 424.

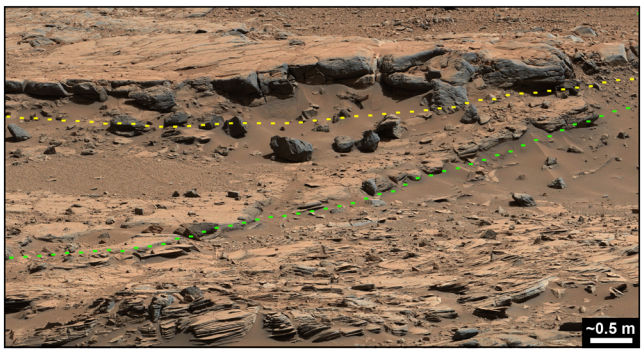

Figure 11. Approximate contact of different facies at Cooperstown (Mastcam mosaic acquired on sol 439). Cross-bedding is evident in the foreground. Image credit: NASA/JPL-Caltech/MSSS.

3.4. Additional APXS Results Along the RTR

The APXS examined 19 targets over sols 360–500, primarily at the Darwin and

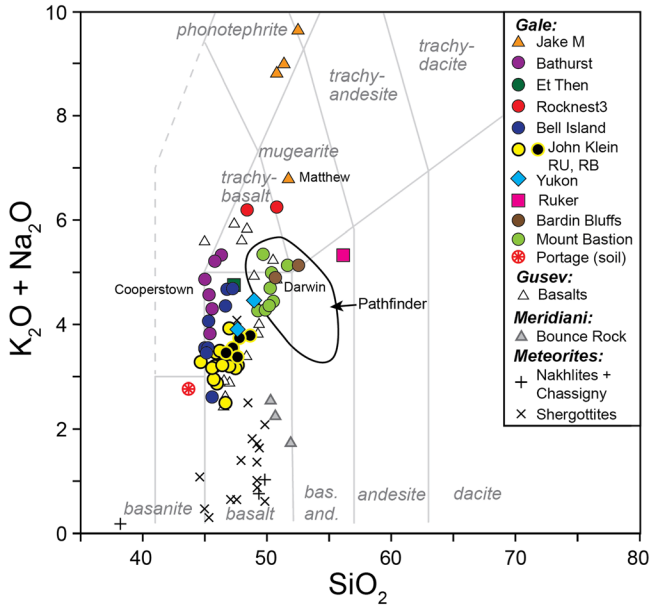

Figure 12. Total alkali versus silica diagram for APXS analyses of Gale rock classes to sol 500 (recalculated to be S and Cl free), SNC meteorites, and select landed mission data sets, as modified from *Schmidt et al.* [2014a]. Symbols reflect interpreted origin, with triangles = volcanic, circles = sedimentary, squares = unknown origin, and diamond = regolith. RU and RB are unbrushed and brushed analyses. The targets at Darwin are classified as Bardin Bluffs and Mount Bastion. The targets at Cooperstown are classified as Bathurst.

Cooperstown waypoints (discussed above). In addition, the APXS examined three targets of opportunity along the RTR and acquired multiple measurements of the cached Cumberland drill sample after it was dumped. The APXS compositions of rock surfaces are similar to those examined earlier along the traverse, allowing us to group them into classes.

The first target of opportunity was a float rock target named "Matthew" (sol 360). Matthew has relatively high alkali (4.8 wt% Na_2O) and Al_2O_3 (13.8 wt%) concentrations like the mugearitic target, Jake Matijevic, examined on sol 46 (Figure 12) [*Stolper et al.*, 2013]. Similarity between these two rock targets indicates that Jake-class rocks are dispersed along the HP unit.

An APXS raster on the Cumberland dump pile confirms the composition of the powdered sample analyzed by SAM and CheMin. In particular, the campaign confirmed the K_2O content (0.62 ± 0.04 wt%, 2σ error) used for K-Ar dating by *Farley et al.* [2014].

Rock compositions from sols 360 to 500 largely reflect their igneous protolith compositions. Differences in K_2O contents along the rover's traverse most likely reflect varying input of alkali-rich and alkali-poor basaltic materials. In addition, we find that minor and trace species (K, Cr, Ni, and Zn) that are detectable and well quantified by APXS are useful discriminators between the Gale rock classes because they are more variable than the major elements, particularly among the more mafic classes [*Schmidt et al.*, 2014b].

3.5. Discussion of RTR Science Results

The presence of sandstones and pebbly sandstones with grain-supported textures and the common presence of cross-stratification both provide strong evidence for a hypothesis of bedload sediment transport in an ancient fluvial system. The heterogeneous grain types are suggestive of a sediment source in the crater rim. In particular, the presence of clasts comprising multiple-fractured grains set in a very fine-grained (potentially glassy) matrix indicates that at least the larger clasts in this outcrop (those for which we can resolve internal structure) are possibly derived from erosion of an impact breccia deposit, the exact source of which is not known. The grain size and scale of cross-stratification at the three contact sites imply sediment transport and deposition by unidirectional currents in a fluvial sedimentary environment [*Edgar et al.*, 2014; *Gupta et al.*, 2014]. Some of the flows were likely vigorous; for example, moderately rounded, pock-marked pebbles at Darwin (Figure 9) are evidence for bedload collisions in high-energy flows [*Williams et al.*, 2014; *Yingst et al.*, 2014]. Average clast roundness differs between the facies, and there are potential differences in sorting, both of which indicate that sediment in each target may have a different transport history. The low to moderate level of rounding is consistent with a high-energy, intermittent transport event such as deposition in an alluvial fan environment [*Williams et al.*, 2013, 2014].

There is abundant evidence for an extensive diagenetic history and widespread burial of the deposits on the Bradbury Rise. The presence of well-cemented sandstones together with mineral-filled veins that cross-cut sedimentary units provide evidence for multiple phases of postdepositional subsurface fluid flow.

Burial depths are unconstrained but had to be sufficient to result in substantial fracturing, followed by precipitation of minerals in veins. The fracture set at Darwin reflects a well-lithified substrate subjected to a tensile stress field presumably associated with lithostatic pressure created during burial.

Despite the abundant textural evidence for fluvial transport and deposition in the various sedimentary facies observed along the RTR, geochemical evidence for aqueous alteration is sparse. Hydrogen is observed by ChemCam and can be linked to hydrous minerals. Whether these minerals formed in situ, such as the cements, is not known. Over the roughly 1000 locations sampled by ChemCam between sols 320 and 500, no calcium sulfate was detected other than at Tingey, including at the waypoint outcrops, Darwin and Cooperstown.

The lack of elemental evidence for chemical weathering does not necessarily constrain mineralogical alteration, however. As argued for the sediments transported to Yellowknife Bay, chemical weathering resulting in significant elemental mobility would be suppressed within a fluvial system characterized by rapid erosion and limited transport (as may be the case for sediments transported from the crater rim) and by cold temperatures [*McLennan et al.*, 2014].

The HP sediments studied along the RTR mostly lack obvious signs of sulfate-involved, late-stage diagenesis. In contrast, calcium sulfates were found by ChemCam in the Yellowknife Bay fluviolacustrine sediments as veins and filled "hollow nodules" [*Grotzinger et al.*, 2014; *Vaniman et al.*, 2014; *Nachon et al.*, 2014]. These calcium sulfates precipitated within fractured sedimentary rock well after their cementation, associated with a late-stage diagenetic phase [*Grotzinger et al.*, 2014; *McLennan et al.*, 2014; *Nachon et al.*, 2014]. This implies that either the late-stage diagenetic episode observed at Yellowknife Bay was less pervasive within hummocky plains rocks or perhaps the Yellowknife Bay rocks are stratigraphically older.

We note that the science team chose not to acquire samples of rocks or soil in this section of the RTR, in order to make progress toward Mt. Sharp. Without the X-ray diffraction and pyrolysis analyses from the onboard laboratories, we rely on elemental chemistry from ChemCam and APXS. At Yellowknife Bay, the geochemistry alone did not provide evidence for chemical weathering of the sediments within the Sheepbed mudstone. Instead, it is likely that the diagenetic processes that led to the formation of phyllosilicates within the Sheepbed mudstone did not noticeably influence bulk rock composition [*McLennan et al.*, 2014], implying low water/rock ratio in postdepositional fluvial activity. As described in section 2, the team has allocated time for one sample acquisition along the RTR, providing an opportunity to measure any isochemical weathering within those sample materials.

Observations throughout the Yellowknife Bay area, as well as those along the HP and RT units, demonstrate a repeated pattern of resistant capstones underlain by less-resistant strata, an arrangement that is susceptible to undermining and scarp retreat. Aeolian erosion exploits the weaker, finer-grained facies producing benches and overhangs of the overlying, coarser-grained facies. This scenario is consistent with the recent exposure ages [*Farley et al.*, 2014] of exhumed rocks at Yellowknife Bay. Collectively, these observations provide criteria for a sampling strategy for rocks with minimal surface exposure ages and therefore greater potential for preserving organic material. Future activities by *Curiosity* will test this idea.

4. Mission Operations and Science Planning

4.1. Planning Timeline and Available Planning Cycles

Mission and science operations generally progressed as described in *Grotzinger et al.* [2012]. The science and engineering teams operated on "Mars Time" for the first 90 sols, with shift times starting approximately 40 min later each day, to provide the maximum amount of time between the receipt of the previous sol's data and the deadline to uplink the next sol's commands. By operating this way, 7 days a week, the team also maximized the number of planning cycles; uplink was possible every sol on Mars. Approximately 280 science team members from around the world were resident at Jet Propulsion Laboratory (JPL) at the start of the surface mission, allowing operations meetings to be held face to face. On any given sol, about 100 science team members participated in operations and 150 attended daily science discussions.

On sol 90, the operations schedule moved to "Earth Time," meaning shift start times started no earlier than 6 A.M. and ended no later than 11 P.M. (Pacific). That schedule required an 11 h planning timeline in order to stay in sync with Mars for about half of the 37-sol Earth-Mars phasing cycle (midnight on Earth and

Mars align every ~37 sols). The remaining sols, called "restricted sols," required planning with data from two sols before. Planning still occurred for each sol, but activities that required knowledge of the state of the rover (such as choosing targets at a new location after a drive or driving consecutively) could be planned only after waiting a sol. Also, beginning sol 90, science team members returned to their home institutions and operations meetings were conducted via telecon and Web-based screen sharing. Secure online chat room discussions, email, information exchange on computer servers, and telecons took the place of face-to-face meetings.

Prior to landing, the goal was to begin developing three-sol plans on Fridays starting at sol 180, freeing the team from working weekends. If a significant change to the rover state were included in these weekend plans (e.g., a drive or arm motion), the remainder of the weekend plan would essentially become restricted (i.e., constrained to activities not dependent on knowledge of the rover state), even if the weekend occurred in an otherwise unrestricted period. In practice, the team went to 6 day/week operations on sol 180 (two-sol plans on Saturdays), and 5 day/week operations after sol 231 (three-sol plans on Fridays), primarily to retain higher productivity while drilling at John Klein. Planning continued at 5 days/week up to and beyond sol 500.

As the planning timeline per sol shortened, less time was available for downlink assessment, activity planning, and sequence generation and validation. Certain coordination meetings were removed as planned in order to streamline the tactical process [*Grotzinger et al.*, 2012]. These limitations were somewhat compensated for by increased efficiency and experience, though other factors affected the overall pace of operations (section 5). Furthermore, progress on complex activities such as driving or sampling is strongly correlated with the number of unconstrained planning cycles available (i.e., those with data available from prior activities), due to both the time needed for planning and steps that require assessment on Earth before proceeding. The percentage of sols that were available as unconstrained planning cycles was 100% through sol 90, 75% through sol 180, 64% through sol 231, and 57% thereafter.

4.2. Hierarchical Science Planning and Prioritization

With a rover as capable and sophisticated as *Curiosity*, and with a landing site as rich as Gale Crater, the variety of potential observations and experiments far exceeds the available resources each sol, and over the mission as a whole. Further, the complexity of operations (e.g., technical constraints, balancing resources across the rover and between sols, and interdependencies of various activities, discussed further in section 5) requires careful and advanced planning to efficiently achieve science objectives. These factors, fully realized only through experience after landing, led to the evolution of a hierarchical science planning structure.

4.2.1. Strategic Planning

While maintaining flexibility to adapt to discoveries, strategic-scale planning (over tens to hundreds of sols) was necessary to determine the pace of progress needed to meet mission objectives, both to provide a focus to the planning and to assess the viability of various mission scenarios. Early in the mission, the team set a sol-specific goal for reaching Glenelg (i.e., the drill target at Yellowknife Bay) and monitored progress each sol. While somewhat arbitrary, the deadline served as a daily reminder of the cost of stationary activities (including unforeseen delays and anomalies) versus driving. Throughout the mission, the team has kept a detailed strategic plan for reaching the base of Mt. Sharp, accounting for days without planning, restricted periods, holidays, rover maintenance activities, seasonal effects, etc. Similar to prelanding mission performance exercises [e.g., *Grotzinger et al.*, 2012], this type of planning initially is used to determine what goals and timelines are realistic. As the Project and science team concur on a choice of goal(s), it then may be used to monitor progress. Interim goals are reviewed and adapted to meet longer-term mission goals, as needed.

To ensure that the planning conforms to operational constraints and remains consistent with overall mission goals, strategic planning is performed jointly with the project system engineers and project management. For the traverse to Mt. Sharp, options were developed and discussed with the science team by members of a working group named "Mt. Sharp or Bust." Finally, the Project Science Group, composed of the Project Scientist, Program Scientist, instrument Principal Investigators, and their deputies, communicates and reinforces the strategic goals by providing written guidance to the wider team that appears in the Long Term Planner's (LTP) daily report.

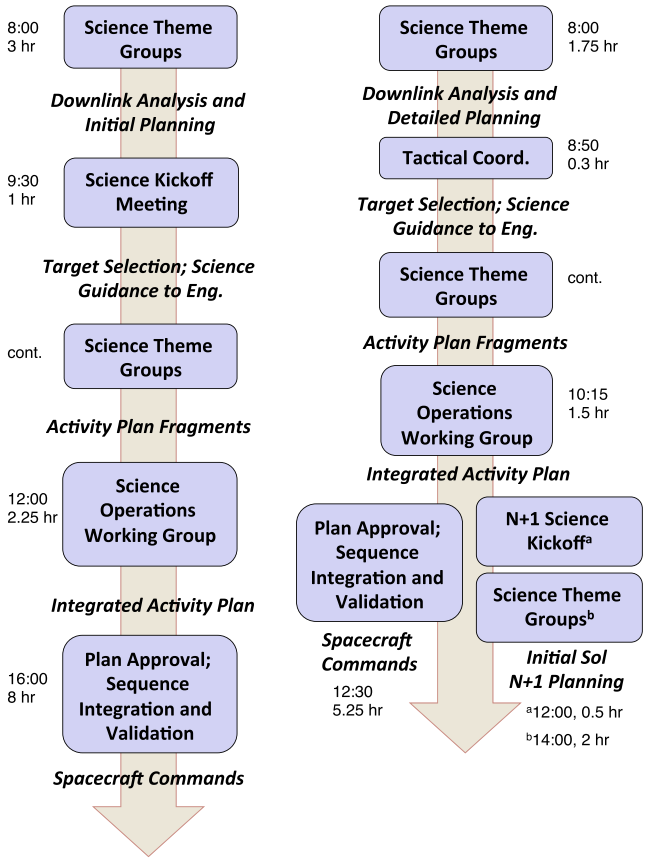

Figure 13. Tactical planning flow (left) during the first 180 sols (16 h) and (right) after re-structuring in May 2013 (9.75 h). The Science Kickoff Meeting was deleted after sol 90, in order to reduce the tactical planning timeline, and replaced with a brief Tactical Coordination Meeting. A new set of meetings was added (Sol $N+1$ Science Kickoff and STG) to add back time for early planning, now done one sol ahead. The meeting start time and duration are listed. The start of the tactical planning cycle is shown here as 8:00 A.M., though it slides in practice.

4.2.2. Supratactical Planning

This term refers to planning that looks roughly 2–10 sols ahead. It has proven key to the efficient operation of *Curiosity* due to the number of factors that must converge over this time scale. For example, mission resources (e.g., energy, telecom rates, and schedules) and near-term science objectives (e.g., details of SAM experiment and resource usage, and progress toward next drive goal) often lack definition until several sols before execution. Because such factors can be highly interdependent (e.g., low telecom rates on sol N may fail to deliver the images needed to drive on sol $N+1$) or require advanced planning (e.g., run a sample cup preconditioning activity a sol before a sample delivery to SAM), initial work to lay out a supratactical plan can avoid losing many sols of productivity over the life of the mission. A team of system engineers leads this process, along with an LTP provided by the science team, and other team members as needed for consultation. The work is done each planning day but offline from tactical operations. Because the LTP is typically rotated every few sols, it also has been helpful to appoint a specific team member to lead campaigns, such as the detailed study of a particular outcrop, in order to provide a single point of contact and "corporate memory" over several weeks.

4.2.3. Tactical Planning

Early in the mission, the science team was divided into three Science Theme Groups (STGs) for planning: geology (GEO), mineralogy/geochemistry (MIN), and environment/atmosphere (ENV). At the beginning of each planning day, these groups assessed the most recent data and generated ideas for the sol being planned (Figure 13). These rough ideas were discussed with engineers at a Science Kickoff Meeting in order to get an initial reading on their viability relative to rover resources. Specific targets for arm placement or drives also were presented so that Rover Planners (RPs) could begin their work. Each STG then finalized its planning and submitted an activity plan fragment via a project-wide planning software tool. The Science Operations Working Group meeting brought STG and instrument representatives together with rover engineers and project management, with the goal of creating an integrated plan (from the STG fragments combined with other engineering activities) for the sol that met safety and resource constraints. The remainder (about half) of the 15 h planning cycle was dedicated to finalizing this plan, developing and validating command sequences, and integrating them into a final master sequence.

As the daily timeline shrank from 15 to 11 h, the team found that the 1–2 h each morning dedicated to the initial science plan development was not enough to thoughtfully consider recent results, discuss options for the sol, and receive guidance from supratactical planners. Starting in May 2013, the science team reorganized the planning timeline to begin midway through the day before (Figure 13). Although the sol N plan had not yet been uplinked, part of the team that just finished developing it could begin to outline a

plan for sol $N+1$ before finishing for the day. A schedule was devised that allowed for an "$N+1$ Science Kickoff" with a supratactical representative and under the direction of the tactical science lead while only minimally impacting the ongoing sol N planning. STGs (now consolidated into GEO-MIN and ENV) then met to begin initial work on their sol $N+1$ plan fragments. This departure from the earlier process, and that used by the Mars Exploration Rover team [*Crisp et al.*, 2003], reflects the increased scope and complexity of *Curiosity*'s operations. The kickoff meeting is open to the entire science team and occurs at the beginning of the team-wide daily science discussion.

The Mission Managers, Project Scientist, and Deputy Project Scientists participated in all levels of planning in order to provide continuity. Further, each planning level documented and communicated its work to the others. For example, strategic planning updates were provided to the Project and team each week. The LTP and supratactical system engineers updated the tactical operations team every sol.

4.3. Specialized Roles for Science Team Members

Each sol, there are a number of roles staffed by project engineers and science team members needed to accomplish the tactical, supratactical, and strategic planning. Most fall into two categories: leadership roles that span the entire rover or payload and roles that cover specific rover subsystems or payload instruments. These largely follow previous rover missions [e.g., *Crisp et al.*, 2003]. A few additional roles, customized to the nature of this mission, evolved during operations tests and while operating *Curiosity* on Mars. These roles provide key scientific expertise to engineers who operate *Curiosity* and its scientific tools, following the highly successful process of "embedding" scientists with the engineering teams during the mission's earlier phases [e.g., *Vasavada*, 2009].

A team of Surface Properties Scientists (SPSs), composed of geologists with special expertise in the mechanical behavior of surface materials, advises the RPs each sol on the potential slip and mobility hazards inferred from rover images and other data. They also refine the strategic drive route (planned on orbital images) as on-the-ground data are available. The SPSs are trained in the mechanical behavior of the rover and the tools used by the RPs to plan drives and arm motions. A team of Surface Sampling System (SSS) Scientists advises the RPs and SSS engineers on the safety (e.g., risk of tool wear, sticking, or clogging) of potential drilling or scooping targets based on contact science data, load testing with the drill prongs, etc. Scientists in this role were involved in extensive prelanding tests of the sampling system on various geologic materials and/or have a strong understanding of composition and potential evolution of samples under temperature or pressure, for example. The SSS Scientists are trained in the mechanics and constraints of the sampling system and provide this knowledge to the wider team as targets are being considered. Typically one SPS and one SSS scientist are on duty each sol.

5. Mission Performance

5.1. Operations Complexity

A recurring theme among scientists, engineers, and managers alike during the first 500 sols of *Curiosity*'s operations was a realization of the complexity of the rover, its payload, and the mission. The complexity comes from a variety of sources, including the number of payload instruments; the sophistication of several of these instruments and the software to operate them as compared to previous rover missions; the variable planning cycles; the many steps involved in acquiring, processing, delivering, and analyzing solid samples; the shifting constraints imposed by available energy, downlink or storage data volumes, or time; and unforeseen anomalies (the risk of which is a function of complexity). These interdependencies have at times resulted in plans that are highly optimized (i.e., success oriented), such that even small problems late in the planning had nonlinear penalties in productivity.

For example, three-sol weekends often are used to accomplish activities too time or energy intensive for a single weekday planning cycle. If an otherwise minor anomaly is detected during the Friday planning cycle, it can cause a loss of three sols of productivity (or more if the effects ripple into the week ahead). As another example, there are intentional break points between arm, mobility, and sampling activities to allow safety checks, following protocols established prior to landing. One such check is a mandatory assessment of the rover's stability and risk of slippage before any arm deployment. This assessment requires the latest

rover data and typically occurs just as the arm activities are being prepared for uplink. If the assessment result is a "no-go," a delay of at least one sol to reposition the rover is required.

Complexity must be identified and managed across all aspects of the planning. The science team may have the time to develop an activity plan that analyzes a number of contact science targets. But the nature of those targets (e.g., their geometries convolved against the 5 degree-of-freedom arm and large drill/instrument turret) may require more time than available for the RPs to create command sequences. Even if the science team and RPs can pull it off, the commands may be too voluminous to be reviewed in the time available before uplink. The latter is especially detrimental since it occurs last in the planning cycle, offering the least time to recover.

Early in the mission, there was a sense of being "nibbled to death by ducks" when the above, as well as a string of one-time issues (e.g., instrument anomalies, telecom losses, ground system problems, and unexpected hardware behaviors), all incrementally degraded productivity. The Project subsequently focused attention on reducing complexity and managing the inherent risks. Steps included moderating the volume of requested science activities, de-coupling activities that may create interdependencies, using supratactical planning to do advance work on drive and arm motions, and developing complexity guidelines and template-based activities, based on experience of what comprises a realistic scope of activities on any given sol. Naturally, the science team desires to accomplish as much as possible, but thoughtful discussions and compromises have preserved productivity while limiting frustration of failed plans (or long hours, or time-stressed planning) and while still preserving the Project's conservative risk posture. Anomalies are more difficult to address, but their frequency has been reduced by refresher training on processes and procedures (to mitigate human error) and team-wide education on what activities or rover situations may be more risk prone.

5.2. Loss of Science Productivity

Through sol 500, 17 sols were completely lost due to anomalies in the planning process, an instrument, or the rover that could not be resolved prior to the next uplink. In addition, one sol each was lost due to an issue with the Deep Space Network, an emergency issue with a key staff member, and the desire to not plan activities during a solar coronal mass ejection. A similar number of sols (20) had only minimal success, such as when a drive faulted well short of its goal or when the primary activity failed but secondary activities succeeded. Considering the above, 92% of sols met or nearly met their immediate goal (without distinguishing whether the goal was science, engineering, or related to a previous anomaly).

Science activities were curtailed on a number of sols, either by design (e.g., for commissioning, FTAs, or during holidays or solar conjunction) or due to anomalies. For example, a few sols were required to investigate foreign object debris at Rocknest before sampling could proceed and to study unexpected behaviors of sample material on the observation tray and within the CheMin instrument. Recovery from the sol 200 anomaly (corruption of the memory on the A-side computer that also exposed underlying software problems) required a few weeks to transition to the B-side computer, complete the investigation of the A-side computer, patch the software, and address a previously undetected anomaly in the B-side Navcams. The Navcam issue itself slowed drive progress for a number of weeks while a solution was tested and validated. The flight software transition starting on sol 444 was unsuccessful, causing several sols to be lost to the failed attempt and the subsequent investigation and recovery. While difficult to quantify, the above suggests that the number of sols successfully used for critical science activities is significantly less than 92%.

5.3. Comparison With Prelanding Expectations

While quantitative mission performance studies were conducted prior to landing as a validation exercise [e.g., *Grotzinger et al.*, 2012], the flexibility to adapt to discoveries as they occurred was always intended. The decision to explore Yellowknife Bay is a prime example. *Curiosity*'s first drives were *away* from its primary science target (Mt. Sharp), delaying its arrival there. This decision was justified by the insights provided by the detailed geologic mapping of the landing area in the weeks before and just after landing [*Grotzinger el al.*, 2014]. The scientific analyses conducted within Yellowknife Bay resulted in the identification of a habitable environment [*Grotzinger*, 2014; *Grotzinger et al.*, 2014], fulfilling the primary science objective of the mission. Exploration of the lower reaches of Mt. Sharp remains the centerpiece of the mission at Gale Crater, given the presence of a rich and diverse stratigraphic sequence that may hold clues to major

environmental transitions in Mars' history, including environments favorable for habitability. These studies will take place largely in the extended mission.

Through sol 360, *Curiosity* had acquired and scientifically analyzed four solid samples (two scoop samples at Rocknest plus drill samples at John Klein and Cumberland) and had driven just under 2 km, compared with the prelanding performance estimate of four samples and 9 km of traverse (at sol 360). The discrepancy in the traverse distance (without being offset by an increase in sampling) suggested that mission performance was somewhat less than anticipated when using these coarse metrics. A project review held in August, 2013, considered potential causes and suggested ways to improve mission return going forward. Causes of the discrepancy in the predicted versus actual performance included the additional time spent exploring Yellowknife Bay (due to its demonstrably high science value), an underestimation of the time needed to complete FTAs (especially those related to sampling), and the anomalies and complexity issues described above. The impact of the sampling FTAs is a consequence of how the test strategy evolved prior to landing. Testing of higher-level rover functions was deferred in order to focus limited time on testing landing and CAP activities and on mitigating significant problems in the rover's avionics and sample contamination control.

Science scope also grew relative to prelanding plans, as the understanding of instrument strategies and capabilities matured. For example, a complete, initial assessment of solid samples with SAM has required multiple sample deliveries (from a single cache of acquired sample material) and evolved gas analyses [*Leshin et al.*, 2013; *Ming et al.*, 2014], relative to the single dropoff and analysis bookkept prior to landing. This is consistent with the way that geochemical laboratories operate on Earth. This in turn led to a realization that if the rover could perform additional contact science and/or drive while holding a cache of sample material, it could be productive while waiting for the laboratory analyses to complete. The tools, processes, and training necessary to provide this capability were developed in parallel with ongoing surface operations, beginning at Rocknest. Operating with a sample cache adds significant complexity due to imposed constraints on mobility and arm motions, requiring detailed planning by specially trained staff, but has increased mission science return.

One high-leverage recommendation from the August review that was immediately adopted was the development of tools and processes to allow *Curiosity* to drive on more sols. This can be done in a way that is independent of the number of unconstrained planning cycles. For example, on benign terrain, the rover can be commanded to use its autonavigation capability to drive on multiple sols without updates from engineers on Earth. This capability will improve drive performance over weekends and restricted sol periods. Drive progress also can be improved by adding more unconstrained planning cycles, either by working on some weekend days or by shortening the planning timeline to extend the unrestricted sol period.

The productivity of the science payload has generally exceeded prelanding expectations (which held conservative margins on time, energy, and data volume). The multiple portions analyzed by SAM per acquired sample, as noted above, is an example. More SAM atmospheric analyses have been accomplished than predicted. Mastcam and ChemCam have been used for remote sensing on many more sols than anticipated, with ChemCam measuring chemical composition at ~2500 observation points on 338 targets during the first year of operations. The MAHLI has proven useful for landscape imaging, self-portraits, wheel wear analyses, and undercarriage inspections, in addition to providing images with a range of geometries and spatial resolutions for contact science. MARDI has been used for surface clast surveys. REMS, RAD, and DAN have acquired a volume of environmental monitoring data well above prelanding expectations (section 2.8).

5.4. Concern Over Wheel Damage

As this article goes to press, *Curiosity*'s engineering and science teams are evaluating an increase in the rate of damage observed on the rover's wheels. While damage was expected, the rate of dents, punctures, and tears in the aluminum wheels has increased notably since sol ~400, as observed using MAHI, Mastcam, and Navcam. In response, teams have been formed to investigate the mechanical properties of the wheels and the dynamics of the mobility system when interacting with rough terrain; to map terrain textures from orbital and rover imagery; and to conduct experiments using flight-like wheels and rover testbeds. While the investigations are ongoing, drive distances have been limited to the stereo Navcam coverage acquired after

Table 2. Schedule for MSL Archive Delivery and Release

Release	Sol Range	Delivery to PDS	Age of Data at Delivery	PDS Release to Public
1a-Experiment Data Records	0–89 (90 sols)	6 Feb 2013	3–6 mo.	27 Feb 2013
1b-Reduced Data Records	0–89 (90 sols)	7 Mar 2013	4–7 mos.	20 Mar 2013
2	90–179 (90 sols)	20 May 2013	3.5–6.5 mos.	10 Jun 2013
3	180–269 (90 sols)	9 Aug 2013	3–6 mos.	30 Aug 2013
4	170–359 (90 sols)	15 Nov 2013	3–6 mos.	13 Dec 2013
5	360–449 (90 sols)	24 Feb 2014	3.5–6.5 mos.	17 Mar 2014
	Plan for Future Deliveries			
6	450–583 (134 sols)	3 Jul 2014	3–8 mos.	1 Aug 2014
7	584–707 (124 sols)	3 Nov 2014	3–7 mos.	5 Dec 2014
8	708–804 (97 sols)	16 Feb 2015	3–6.5 mos.	16 Mar 2015
9	805–938 (134 sols)	3 Jul 2015	3–8 mos.	31 Jul 2015
10	939–1062 (124 sols)	2 Nov 2015	3–7 mos.	5 Dec 2015
11	1063–1159 (97 sols)	17 Feb 2016	3–6.5 mos.	16 Mar 2016
12	1160–1293 (134 sols)	1 Jul 2016	3–8 mos.	1 Aug 2016
13	1294–1417 (124 sols)	31 Oct 2016	3–7 mos.	5 Dec 2016
14	1418–1514 (97 sols)	16 Feb 2017	3–6.5 mos.	16 Mar 2017
15	1515–1648 (134 sols)	3 Jul 2017	3–8 mos.	1 Aug 2017

each prior drive (~20–30 m), allowing manual route planning and rock avoidance. Autonavigation and multi-sol driving were disallowed. These limitations have significantly degraded the drive progress toward Mt. Sharp but should eventually be relaxed as new route planning and drive protocols are established in response to the findings of the investigations.

6. Naming Conventions

Gale Crater, Aeolis Mons, and Peace Vallis are names adopted by the International Astronomical Union (IAU). Mt. Sharp is an informal name for Aeolis Mons recognizing Robert P. Sharp, a geologist who made key contributions to early Mars exploration. Bradbury Landing recognizes the author Ray Bradbury. The first rock chosen for contact science was named in honor of Jacob Matijevic, a lead engineer on all of NASA's Mars rover missions. The first rock drilled by *Curiosity* was named in honor of John W. Klein, a former Deputy Project Manager for MSL. The entry point to Mt. Sharp (Murray Buttes) was named in honor of Prof. Bruce Murray of Caltech, a pioneer of the early scientific missions to Mars.

Throughout the early mission, *Curiosity* operated within the Yellowknife quadrangle on the geologic map created by the science team prior to arrival [*Grotzinger et al.*, 2014] and named after the IAU-designated Yellowknife Crater within the quad. Science targets within the quad are named following the Yellowknife theme, after the city in northern Canada that was the starting point for many significant geologic expeditions investigating ancient Archean deposits. Similarly, Darwin falls within the Mawson quadrangle, which Curiosity entered on sol 371. Mawson, Antarctica, is the oldest operating base within the Antarctic circle and is named after the Antarctic geologist and explorer Sir Douglas Mawson. Cooperstown is located within the Coeymans quadrangle that takes its name from the town of Coeymans in upstate New York, located near the fossil-rich Coeymans Limestone Formation. Names relevant to the Coeymans quadrangle were used starting on sol 417. Within all quadrangles, science target names derive from rock formation names, which in turn derive from local geographic names.

7. Planetary Data System Archive

The MSL Project generates, validates, and delivers the mission's raw and derived data sets (called Experiment Data Records and Reduced Data Records, respectively) to the Planetary Data System (PDS) in batches 3 to 4 times a year according to the schedule shown in Table 2. The data products archived are listed in Table 3. The products and ancillary supporting information can be found at the following PDS online archives: APXS, ChemCam, CheMin, DAN, and SAM at the Geosciences Node; Hazcam, Navcam, MAHLI, MARDI, and Mastcam at the Imaging Node; RAD at the Planetary Plasma Interactions Node; REMS at the Atmospheres

Table 3. List of Archived MSL Data Products

Instrument	Data Products
APXS	raw data, summed X-ray spectra, wt. % elemental oxide abundance
ChemCam	raw data, Level 1 LIBS data, Level 2 LIBS major element compositions, RMI images processed to remove artifacts
CheMin	raw data, diffraction data as 2-theta versus intensity, energy dispersive histograms, and mineral identification and abundances
DAN	raw data, reduced passive neutron data, reduced active neutron data, averaged reduced passive neutron data, and averaged reduced active neutron data
Hazcam, Navcam	raw data, inverse lookup-table scaled images, inverse lookup-table scaled and geometrically linearized images, radiometrically corrected images, stereo disparity and disparity masks, 3D *XYZ* coordinates, surface normal vector maps, surface roughness maps for drill and dust removal tool, range maps, robotic arm reachability maps, slope maps
MAHLI, MARDI, Mastcam	raw data; radiometrically calibrated data; radiometrically calibrated and color corrected data; radiometrically calibrated and geometrically linearized data; and radiometrically calibrated, color corrected, and geometrically linearized data
MAHLI, Mastcam	focus *z*-stack merge images and range maps
RAD	raw data, calibrated data
REMS	raw data; Level 1a calibrated thermal and electrical values from sensors; Level 1b: wind sensor longitudinal/transversal differential thermal conductance, ground temperature sensor brightness temperature, air temperature, ultraviolet sensor radiation, relative humidity, humidity temperature sensor, pressure; Level 1c: ground temperature sensor brightness temperature, local air temperature around each boom and estimated ambient temperature around the rover, ultraviolet radiation for each band and uncertainties, local relative humidity and temperature of the humidity sensor, pressure
SAM	raw data (safed); Level 0 unpacked raw values or counts; Level 1a: QMS mass-to-charge ratio counts per second and RF counts per second, GC Thermal Conductivity Detector gain and offset, TLS direct and harmonic absorption spectra; Level 1b: QMS *m/z* and signal versus time, pyrolysis oven temperature, and gas chromatograph column temperature; GC signal versus retention time, pressure, column temperature, and column used; and TLS direct and harmonic absorption spectra with filtering; Level 2: QMS composition and isotope ratios and gas composition with peak sample temperature for evolved gas analysis (EGA) runs, GC species identified and their relative abundances for pyrolysis products and derivatized compounds, TLS abundances and isotope ratios
SPICE	variety of kernel types including these SPK kernels: cruise trajectory, EDL trajectory, landing site location, rover path and site locations, solar system planets and satellites ephemeris, rover structures and instruments locations

Node; and SPICE information (e.g., kernels and ephemerides) at the Navigation Node. All may be accessed via the PDS home (http://pds.nasa.gov/).

In addition to the PDS online archives, the MSL Analyst's Notebook and Planetary Image Atlas provide alternate ways for users to search and access the data products. The Analyst's Notebook (https://an.rsl.wustl.edu/msl/mslbrowser/) is a user-friendly Web-based tool for correlating data products from various instruments based on time, location, observation target, and other criteria. In addition, detailed views into operational decisions, activity and sequence planning, rover location, and mission history context are unique to the Notebook. Using the Notebook, a scientist can virtually replay mission events to better select and understand data products of interest. The Planetary Image Atlas (http://pds-imaging.jpl.nasa.gov/search/) allows searching and downloading of image products.

Acknowledgments
The MSL Science Team and all those who contributed to the design, development, testing, and operation of MSL are acknowledged for their roles in the mission's success. During early operations, the MSL Project Manager was Pete Theisinger, the Deputy Project Manager was Richard Cook, and the Mission Manager was Mike Watkins. Presently, the Project Manager is Jim Erickson and the Deputy Project Manager is Jennifer Trosper. Nicole Spanovich is the Science Operations Team Chief, and Andy Mishkin leads Integrated Planning and Execution. Part of this research was carried out at the Jet Propulsion Laboratory, California Institute of Technology, under a contract with the National Aeronautics and Space Administration.

References

Anderson, R. C., et al. (2012), Collecting samples in Gale crater, Mars; an overview of the Mars Science Laboratory Sample Acquisition, Sample Processing and Handling System, *Space Sci. Rev.*, *170*, 57–75, doi:10.1007/s11214-012-9898-9.
Anderson, R. B., et al. (2014), ChemCam results from the Shaler outcrop in Gale Crater, Mars, *Lunar Planet Sci.*, *45*, Abstract 2380.
Archer, P. D., Jr., et al. (2014), Abundances and implications of volatile-bearing species from evolved gas analysis of the Rocknest aeolian deposit, Gale Crater, Mars, *J. Geophys. Res. Planets*, *119*, 237–254, doi:10.1002/2013JE004493.

Arvidson, R. E., et al. (2014), Terrain physical properties derived from orbital data and the first 360 sols of Mars Science Laboratory Curiosity rover observations in Gale Crater, *J. Geophys. Res. Planets*, *119*, doi:10.1002/2013JE004605.

Atreya, S. K., et al. (2013), Primordial argon isotope fractionation in the atmosphere of Mars measured by the SAM instrument on Curiosity, and implications for atmospheric loss, *Geophys. Res. Lett.*, *40*, 5605–5609, doi:10.1002/2013GL057763.

Bish, D. L., et al. (2013), X-ray results from Mars Science Laboratory: Mineralogy of Rocknest at Gale Crater, *Science*, *341*, doi:10.1126/science.1238932.

Blake, D., et al. (2012), Characterization and calibration of the CheMin mineralogical instrument on Mars Science Laboratory, *Space Sci. Rev.*, *170*, 341–399, doi:10.1007/s11214-012-9905-1.

Blake, D. F., et al. (2013), Curiosity at Gale Crater, Mars: Characterization and analysis of the Rocknest sand shadow, *Science*, *341*, doi:10.1126/science.1239505.

Campbell, J. L., et al. (2012), Calibration of the Mars Science Laboratory alpha particle X-ray spectrometer, *Space Sci. Rev.*, *170*, 319–340, doi:10.1007/s11214-0129873-5.

Crisp, J. A., M. Adler, J. R. Matijevic, S. W. Squyres, R. E. Arvidson, and D. M. Kass (2003), Mars Exploration Rover mission, *J. Geophys. Res.*, *108*(E12), 8061, doi:10.1029/2002JE002038.

Edgar, L. A., et al. (2014), A fluvial sandbody on Mars: Reconstruction of the Shaler outcrop, Gale Crater, Mars, *Lunar Planet Sci.*, *45*, Abstract 1648.

Edgett, K. S., et al. (2012), Curiosity's Mars Hand Lens Imager (MAHLI) investigation, *Space Sci. Rev.*, *170*, 259–317, doi:10.1007/s11214-012-9910-4.

Farley, K. A., et al. (2014), In situ radiometric and exposure age dating of the Martian surface, *Science*, *343*, doi:10.1126/science.1247166.

Fergason, R. L., P. R. Christensen, M. P. Golombek, and T. J. Parker (2012), Surface properties of the Mars Science Laboratory candidate landing sites: Characterization from orbit and predictions, *Space Sci. Rev.*, *170*, 739–773, doi:10.1007/s11214-012-9891-3.

Fraeman, A. A., et al. (2013), A hematite-bearing layer in Gale crater, Mars: Mapping and implications for past aqueous conditions, *Geology*, *41*, 1103–1106, doi:10.1130/G34613.1.

Glavin, D. P., et al. (2013), Evidence for perchlorates and the origin of chlorinated hydrocarbons detected by SAM at the Rocknest aeolian deposit in Gale Crater, *J. Geophys. Res. Planets*, *118*, 1–19, doi:10.1002/jgre.20144.

Golombek, M., et al. (2012), Selection of the Mars Science Laboratory landing site, *Space Sci. Rev.*, *170*, 641–737, doi:10.1007/s11214-012-9916-y.

Gómez-Elvira, J., et al. (2012), REMS: The environmental sensor suite for the Mars Science Laboratory rover, *Space Sci. Rev.*, *170*, 583–640, doi:10.1007/s11214-012-9921-1.

Grotzinger, J. P., et al. (2012), Mars Science Laboratory mission and science investigation, *Space Sci. Rev.*, *170*, 5–56, doi:10.1007/s11214-012-9892-2.

Grotzinger, J. P. (2013), Analysis of surface materials by the Curiosity Mars Rover, *Science*, *341*, 1457, doi:10.1126/science.1244258.

Grotzinger, J. P. (2014), Habitability, taphonomy, and the search for organic carbon on Mars, *Science*, *343*, 386–387, doi:10.1126/science.1249944.

Grotzinger, J. P., et al. (2014), A habitable fluvio-lacustrine environment at Yellowknife Bay, Gale Crater, Mars, *Science*, *343*, doi:10.1126/science.1242777.

Gupta, S., et al. (2014), An aquatic journey toward Aeolis Mons (Mount Sharp): Sedimentary rock evidence observed by Mars Science Laboratory, *European Geophysical Union*, 2014.

Haberle, R. M., et al. (2014), Preliminary interpretation of the REMS pressure data from the first 100 sols of the MSL mission, *J. Geophys. Res. Planets*, *119*, 440–453, doi:10.1002/2013JE004488.

Hamilton, V. E., et al. (2014), Observations and preliminary science results from the first 100 sols of MSL REMS ground temperature sensor measurements at Gale Crater, *J. Geophys. Res. Planets*, *119*, 745–770, doi:10.1002/2013JE004520.

Harri, A.-M., et al. (2014), Pressure observations by the Curiosity rover: Initial results, *J. Geophys. Res. Planets*, *119*, 82–92, doi:10.1002/2013JE004423.

Hassler, D. M., et al. (2012), The Radiation Assessment Detector (RAD) investigation, *Space Sci. Rev.*, *170*, 503–558, doi:10.1007/s11214-012-9913-1.

Hassler, D. M., et al. (2014), Mars' surface radiation environment measured with the Mars Science Laboratory's Curiosity rover, *Science*, *343*(6169), doi:10.1126/science.1244797.

Johnson, J. R., et al. (2014), ChemCam passive reflectance spectroscopy of surface materials at the Curiosity landing site, Mars, *Icarus*, doi:10.1016/j.icarus.2014.02.028.

Leshin, L. A., et al. (2013), Volatile, isotope, and organic analysis of Martian fines with the Curiosity rover, *Science*, *341*, doi:10.1126/science:1238937.

Mahaffy, P. R., et al. (2012), The Sample Analysis at Mars investigation and instrument suite, *Space Sci. Rev.*, *170*, 401–478, doi:10.1007/s11214-012-9879-z.

Mahaffy, P. R., et al. (2013), Abundance and isotopic composition of gases in the Martian atmosphere from the Curiosity rover, *Science*, *341*, 263–266, doi:10.1126/science.1237966.

Maurice, S., et al. (2012), The ChemCam instrument suite on the Mars Science Laboratory (MSL) rover: Science objectives and mast unit description, *Space Sci. Rev.*, *170*, 95–166, doi:10.1007/s11214-012-9912-2.

McAdam, A. C., et al. (2014), Sulfur-bearing phases detected by evolved gas analysis of the Rocknest aeolian deposit, Gale Crater, Mars, *J. Geophys. Res. Planets*, *119*, 373–393, doi:10.1002/2013JE004518.

McLennan, S. M., et al. (2014), Elemental geochemistry of sedimentary rocks at Yellowknife Bay, Gale Crater, Mars, *Science*, *343*, doi:10.1126/science.1244734.

Meslin, P.-Y., et al. (2013), Soil diversity and hydration as observed by ChemCam at Gale Crater, Mars, *Science*, *341*, doi:10.1126/science.1238670.

Ming, D. W., et al. (2014), Volatile and organic compositions of sedimentary rocks in Yellowknife Bay, Gale Crater, Mars, *Science*, *343*, doi:10.1126/science.1245267.

Minitti, M. E., et al. (2013), MAHLI at the Rocknest sand shadow: Science and science-enabling activities, *J. Geophys. Res. Planets*, *118*, 2338–2360, doi:10.1002/2013JE004426.

Mitrofanov, I. G., et al. (2012), Dynamic Albedo of Neutrons (DAN) experiment onboard NASA's Mars Science Laboratory, *Space Sci. Rev.*, *170*, 559–582, doi:10.1007/s11214-012-9924-y.

Nachon, M., et al. (2014), Calcium sulfate characterized by ChemCam/Curiosity at Gale Crater, Mars, *Lunar Planet Sci.*, *45*, Abstract 2006.

Ollila, A. M., et al. (2014), Trace element geochemistry (Li, Ba, Sr, and Rb) using Curiosity's ChemCam: Early results for Gale crater from Bradbury Landing Site to Rocknest, *J. Geophys. Res. Planets*, *119*, 255–285, doi:10.1002/2013JE004517.

Sautter, V., et al. (2014), Igneous mineralogy at Bradbury rise: The first ChemCam campaign at Gale crater, *J. Geophys. Res. Planets*, *119*, 30–46, doi:10.1002/2013JE004472.

Schmidt, M. E., et al. (2014a), Geochemical diversity in first rocks examined by the Curiosity rover in Gale crater: Evidence for and significance of an alkali and volatile-rich igneous source, *J. Geophys. Res. Planets*, *119*, 64–81, doi:10.1002/2013JE004481.

Schmidt, M. E., et al. (2014b), Geochemical classification of rocks in Gale Crater with APXS to sol 360: Sediment provenance, mixing, and diagenetic processes, *Lunar Planet. Sci.*, *45*, Abstract 1504.

Stolper, E. M., et al. (2013), The petrochemistry of Jake_M: A Martian mugearite, *Science*, *341*, doi:10.1126/science.1239463.

Vaniman, D. T., et al. (2014), Mineralogy of a mudstone at Yellowknife Bay, Gale Crater, Mars, *Science*, *343*, doi:10.1126/science.1243480.

Vasavada, A. R. (2009), Mars Science Laboratory: Integrating science and engineering teams, *NASA ASK Magazine*, *34*, 34-37.

Webster, C. R., et al. (2013a), Isotope ratios of H, C, and O in CO_2 and H_2O of the Martian atmosphere, *Science*, *341*, 260–263, doi:10.1126/science.1237961.

Webster, C. R., et al. (2013b), Low upper limit to methane abundance on Mars, *Science*, *342*, 355–357, doi:10.1126/science.1242902.

Wiens, R. C., et al. (2012), The ChemCam instrument suite on the Mars Science Laboratory (MSL) rover: Body unit and combined system tests, *Space Sci. Rev.*, *170*, 167–227, doi:10.1007/s11214-012-9902-4.

Wiens, R. C., et al. (2013), Pre-flight calibration and initial data processing for the ChemCam laser-induced breakdown spectroscopy instrument on the Mars Science Laboratory rover, *Spectrochim. Acta B*, *82*, 1–27, doi:10.1016/j.sab.2013.02.003.

Williams, R. M. E., et al. (2013), Martian fluvial conglomerates at Gale Crater, *Science*, *340*, 1068–1072, doi:10.1126/science.1237317.

Williams, R. M. E., et al. (2014), Sedimentology of Darwin waypoint from Curiosity observations, *Lunar Planet Sci.*, *45*, Abstract 2401.

Wong, M. H., et al. (2013), Isotopes of nitrogen on Mars: Atmospheric measurements by Curiosity's mass spectrometer, *Geophys. Res. Lett.*, *40*, 6033–6037, doi:10.1002/2013GL057840.

Yingst, R. A., et al. (2014), Lithology and texture of a potential conglomerate in Gale Crater as imaged by MAHLI, *Lunar Planet Sci.*, *45*, Abstract 1295.